CHARACTERIZATION OF LIVER-SPECIFIC
CHREBP KNOCKOUT MICE

APPROVED BY SUPERVISORY COMMITTEE

Michael S. Brown, M.D.

Joseph L. Goldstein, M.D.

Jay D. Horton, M.D.

Joyce J. Repa, Ph.D.

Jin Ye, Ph.D. (Chair)

DEDICATION

I would like to thank my parents, Kenneth and Alison Linden, for their love and support

CHARACTERIZATION OF LIVER-SPECIFIC CHREBP KNOCKOUT MICE

by

ALBERT GEORGE LINDEN

DISSERTATION THESIS

Presented to the Faculty of the Graduate School of Biomedical Sciences

The University of Texas Southwestern Medical Center

In Partial Fulfillment of the Requirements

For the Degree of

DOCTOR OF PHILOSOPHY

The University of Texas Southwestern Medical Center

Dallas, Texas

May, 2017

Copyright

by

Albert George Linden, 2017

All Rights Reserved

CHARACTERIZATION OF LIVER-SPECIFIC
CHREBP KNOCKOUT MICE

ALBERT GEORGE LINDEN, Ph.D.

The University of Texas Southwestern Medical Center, 2017

MICHAEL S. BROWN, M.D.
JOSEPH L. GOLDSTEIN, M.D.

ChREBP (Carbohydrate Response Element-Binding Protein) and SREBP-1c (Sterol Regulatory Element-Binding Protein-1c) both stimulate the transcription of genes required for lipid synthesis in the liver. My project was designed to investigate the roles of these two factors in regulating the lipogenic pathway. ChREBP and SREBP-1c are induced by carbohydrates, but by different mechanisms. SREBP-1c is stimulated by insulin, while ChREBP is insulin-independent, but dependent on intracellular glucose levels.

This issue was studied previously using mice with a germline deletion in ChREBP, but these experiments were limited because these whole-body ChREBP knockout mice did not tolerate a high sucrose diet. To circumvent this problem, we produced mice with a liver-

specific knockout of ChREBP (*L-ChREBP*$^{-/-}$). When *L-ChREBP*$^{-/-}$ mice were fasted and refed a high-sucrose diet, they consumed a normal amount of food, but lipogenic gene mRNAs were not induced by refeeding. However, this effect could not be solely attributed to the loss of ChREBP because the *L-ChREBP*$^{-/-}$ mice unexpectedly also had reduced levels of nuclear SREBP-1. Previous experiments have shown that SREBP-1c is required for the postprandial induction of lipogenic gene mRNAs in the livers of mice subjected to fasting and refeeding. To determine whether the decreased lipogenesis in *L-ChREBP*$^{-/-}$ mice was caused by reductions in SREBP-1c, ChREBP, or both transcription factors, we injected the *L-ChREBP*$^{-/-}$ mice with an adeno-associated virus encoding the active nuclear form of SREBP-1c. The expression of some lipogenic genes was restored by normalizing the content of nuclear SREBP-1c, but others were not.

Therefore, both SREBP-1c and ChREBP are required for full stimulation of lipogenesis in the postprandial state. Insulin stimulates fatty acid synthesis by activating SREBP-1c. However, glucose is also necessary for lipogenesis, and the additional requirement of ChREBP to induce lipogenic enzymes ensures that the liver will not produce fatty acids unless both insulin and glucose are present.

TABLE OF CONTENTS

PRIOR PUBLICATIONS

McFarlane M.R., Cantoria M.J., Linden A.G., January B.A., Liang G., Engelking L.J., Scap is required for sterol synthesis and crypt growth in intestinal mucosa. *J. Lipid Res.* 2015 April 20.

LIST OF FIGURES

LIST OF TABLES

LIST OF APPENDICES

LIST OF DEFINITIONS

6PGDH – 6-phosphogluconate dehydrogenase

ACC1 – Acetyl-CoA carboxylase 1

ACC2 – Acetyl-CoA carboxylase 2

ACSS2 – Acetyl-CoA synthetase, also known as acetate-CoA ligase or Acyl-CoA synthetase short-chain family member 2

ACLY – ATP citrate lyase

ApoB – Apolipoprotein B

ChREBP – Carbohydrate Response Element-Binding Protein, also known as MLXIPL (Mlx-Interacting Protein-Like)

ELOVL6 – Long-chain fatty-acyl elongase 6

FDPS – Farnesyl diphosphate synthase

FASN – Fatty acid synthase

G6PC – Glucose-6-phosphatase

G6PD – Glucose-6-phosphate dehydrogenase

GPAT1 – Glycerol-3-phosphate acyltransferase 1

HK4 – Hexokinase 4, also known as glucokinase

HMGR – 3-hydroxy-3-methylglutaryl-CoA reductase

HMGS – 3-hydroxy-3-methylglutaryl-CoA synthase

Insig-1 – Insulin-induced gene 1

Insig-2 – Insulin-induced gene 2

LDLR – Low-density lipoprotein receptor

LXR – Liver-X-Receptor

ME1 – malic enzyme 1, NADP(+) dependent

PCSK9 – Proprotein convertase subtilisin/kexin type 9

PKLR – Pyruvate kinase, liver and red blood cell-type

RGS16 – Regulator of G-protein signaling 16

Scap – SREBP cleavage-activating protein

SCD1 – Stearoyl-CoA desaturase 1

SREBP – Sterol Regulatory Element-Binding Protein, also known as SREBF

SQS1 – Squalene synthase 1

CHAPTER ONE
Introduction

REGULATION OF LIPOGENESIS

Purpose of lipogenesis

All organisms experience changes in food availability in their environments. While many species of single-celled organisms are able to enter a quiescent state to await an increase in nutrient availability, organisms of greater complexity require the ongoing utilization of a basal level of metabolic energy to maintain life. This requirement necessitates the ability to store excess calories for future use. In mammals, short-term energy storage is accomplished via the polymerization of glucose molecules to form glycogen, which is stored in the liver and muscle tissue. Long-term energy storage requires the conversion of carbohydrates to triglycerides, which are stored in adipose tissue. In times of extreme starvation, the body can also catabolize the protein in muscle tissue. The objective of my project was to determine which regulatory factor governs each particular enzyme that contributes to the synthesis of fatty acids.

Known transcription factors involved in the regulation of lipogenesis

There are three transcription factors that have been shown to be strongly involved in regulating the expression of lipogenic genes. These three factors are Sterol Regulatory Element-Binding Protein-1 (SREBP-1), Carbohydrate Response Element-Binding Protein (ChREBP), and Liver-X-Receptor (LXR). In addition to regulating lipogenesis, these genes

as a group also regulate aspects of cholesterol and glucose metabolism. All three consist of gene families encoding multiple isoforms (Hua et al., 1995; Herman et al., 2012; Seol et al., 1995). The differing expression of these isoforms among the various tissues of the body allows for the localization of metabolic functions to particular tissues.

Role of SREBP-1 in transcriptional regulation

A 42-base pair direct repeat sequence that confers sensitivity to transcriptional repression by sterols was found in the 5' flanking region of the LDL receptor gene, and was dubbed the sterol regulatory element (Südhof et al., 1987). SREBP-1 was purified in 1993 by isolating a protein fragment that bound to the sterol regulatory element of the LDL receptor (Wang et al., 1993). The full-length precursor to the active, truncated transcription factor was identified shortly thereafter (Yokoyama et al., 1993; Wang et al., 1994). Proteins in the SREBP family (SREBP-1a, SREBP-1c, and SREBP-2) consist of an N-terminal DNA-binding domain that is membrane-tethered by two transmembrane domains as well as a C-terminal regulatory domain (Hua et al., 1996). In the ER, SREBPs interact with another transmembrane protein, the SREBP cleavage-activating protein (Scap) (reviewed in Brown and Goldstein, 1997).

When sterols are absent, the Scap-SREBP complex migrates to the Golgi, where two proteases (site-1 protease and site-2 protease, or S1P and S2P) cleave the N-terminal domain from the transmembrane domains, thus freeing the DNA-binding domain for translocation to the nucleus and the induction of target gene transcription (Nohturfft et al., 1999; reviewed in Brown and Goldstein, 1997). The addition of an ER retention signal sequence to S1P

obviates the need for SREBP transport to the Golgi prior to processing (DeBose-Boyd et al., 1999). The specific amino acid sequence of the first transmembrane segment of SREBPs is also important for its interaction with S2P; the elimination of an NP residue pair abrogated SREBP processing by S2P (Ye et al., 2000). SREBPs are required for the development of fatty liver in obese, insulin-resistant mice; eliminating Scap by gene knockout (leading to a complete loss of nuclear SREBPs) completely abrogated the excess lipogenesis and liver storage of triglycerides found in *ob/ob* mice (Moon et al., 2012). The DNA-binding domain of SREBPs belongs to the basic helix-loop-helix-leucine zipper family (Horton et al., 2002). When oxysterols are present, the Insig family of proteins sequesters the Scap-SREBP complex in the ER, preventing processing (Radhakrishnan et al., 2007; Sun et al., 2007). Overexpression of Insig-1 can also inhibit SREBP processing (Engelking et al., 2004).

The ratio of SREBP-1a to SREBP-1c varies from tissue to tissue (Shimomura et al., 1997), and in the liver SREBP-1c is the primary isoform. SREBP-2 is primarily involved in regulating cholesterol synthesis rather than lipogenesis (Hua et al., 1993). The synthesis of cholesterol is the result of an enzyme pathway that is subject to negative regulation by sterols to avoid the production of excess levels of cholesterol (reviewed in Goldstein and Brown, 1990). Selective knockout of SREBP-1c, leaving SREBP-1a and SREBP-2 intact, led to a decrease in lipogenic mRNA levels; LXR agonists were also less effective at stimulating transcription of lipogenic genes in SREBP-1c knockout mice, suggesting that SREBP-1c is a necessary component of the lipogenic response to LXR activation (Liang et al., 2002). In addition to affecting SREBP-1c transcription by inhibiting the binding of ligands to LXR, polyunsaturated fatty acids were found to induce SREBP-1c mRNA transcript decay, while

having no effect on SREBP-1a mRNA (Xu et al., 2001). SREBP-1c transcription as well as processing is induced by insulin; the proteolytic processing is p70 S6-kinase dependent, while transcription is not (Li et al., 2010, Owen et al., 2012).

Identification of ChREBP and phenotype of knockout

While the involvement of insulin and glucose in regulating carbohydrate metabolism via gene transcription has been known for decades, the identification of the transcription factors involved is a more recent discovery. Immediately upstream of the coding region of the liver-type pyruvate kinase gene (PKLR), the region containing nucleotides -197 to -96 was found to be essential for carbohydrate-dependent regulation of transcription (Thompson and Towle, 1991). Pyruvate kinase catalyzes the final step in glycolysis, and the levels of PKLR enzyme serve as a regulatory mechanism to control the rate of glycolysis in the cell.

A direct C(A/C)CG(G/T)G repeat was later identified as the carbohydrate response element (ChRE) (Liu et al., 1993). ChREBP was purified in 2001 as a protein that bound the ChRE of the PKLR promoter (Yamashita et al., 2001). ChREs are found in the promoters of the PKLR, acetyl-CoA carboxylase 1, and fatty acid synthase genes, where they mediate ChREBP-dependent transcriptional activation under high glucose conditions (Ishii et al., 2004). In addition to stimulating lipogenesis, ChREBP inhibits lipolysis via the upregulation of RGS16 (Pashkov et al., 2011).

A whole-body ChREBP knockout mouse was generated and found to have decreased adipose tissue mass, decreased liver and plasma triglycerides, and increased plasma glucose, consistent with the expected changes secondary to a defect in lipogenesis (Iizuka et al.,

2004). Similar to *ob/ob* mice with a liver-specific Scap deficiency, ChREBP deficiency partially ameliorated the metabolic derangements of double mutant *ChREBP*$^{-/-}$*; ob/ob* mice. (Iizuka et al., 2006). The *ChREBP*$^{-/-}$ mice were also intolerant of a high sucrose diet, exhibiting decreased food intake and hypothermia, which was ultimately lethal. This sucrose intolerance may be due to the decrease in gene transcription of genes involved in fructose metabolism, such as triose kinase and fructokinase. A detailed investigation of the metabolites present in the livers of *ChREBP*$^{-/-}$ mice showed alterations in the cytosolic and mitochondrial [NAD^+]/[NADH] ratios, as well as a decrease in the [ATP]/[ADP][P_i] ratio, indicating that ChREBP deficiency leads to a low-energy state in the liver (Burgess et al., 2008). More recently, ChIP analysis of all ChREBP binding sites in the liver and adipose tissues of mice has shown that metabolic genes contain the highest frequency of ChREBP binding sites in the mouse genome (Poungvarin et al., 2015)

ChREBP isoforms and posttranslational regulation

Recently, a second isoform of ChREBP, ChREBP-β, was discovered (Herman et al., 2012). The possibility of alternatively spliced isoforms of ChREBP products suggests that differential expression of exons could change the localization, protein cofactor binding, or DNA binding activity of ChREBP. ChREBP-β lacks the first exon present in ChREBP-α, and thus does not have the two nuclear export sites and one nuclear import site present at the N-terminal end of ChREBP-α (Fukasawa et al., 2010). The ChREBP-β promoter contains a ChRE, suggesting that ChREBP-β transcription may be induced by high intracellular glucose.

ChREBP is regulated via the phosphorylation of various serine and threonine residues that govern its localization (reviewed in Uyeda and Repa, 2006). Phosphorylation leads to the sequestration of ChREBP in the cytosol, while dephosphorylation leads to nuclear import and the activation of transcriptional activity. cAMP-dependent protein kinase (PKA) phosphorylates Ser-196 and Thr-666 (Kawaguchi et al., 2001). Ser-196 is adjacent to the nuclear localization sequence, and its phosphorylation renders the NLS inactive, enabling protein 14-3-3 binding, which sequesters ChREBP in the cytosol. Dephosphorylation of Ser-196 leads to association with importin-α, which transports ChREBP into the nucleus (Sakiyama et al., 2008). Farther towards the C-terminal end of the protein, Thr-666 is located inside the DNA binding region, and its phosphorylation inhibits DNA binding (Uyeda et al., 2002). Ser-568, located adjacent to the DNA binding domain, is phosphorylated by AMP-dependent protein kinase (AMPK) when fatty acids are abundant in the cell, which also leads to a loss of DNA-binding activity (Kawaguchi et al., 2002). In addition to cellular glucose and its regulation of ChREBP phosphorylation, recently other factors have been found to govern ChREBP activity: ketone bodies inhibit the nuclear import of ChREBP (Nakagawa et al., 2013), and glycosylation was shown to be essential for ChREBP activity (Sakiyama et al., 2010).

A specific member of the PP2A family, PP2A-ABδC, is responsible for dephosphorylation of Ser-196, Ser-568 and Thr-666, and the phosphatase activity is dependent on xylulose-5-phosphate, an intermediate of the pentose phosphate pathway (Kabashima et al., 2003). The pentose phosphate pathway is highly active in the liver and is

responsible for the production of NADPH, which supplies the reducing equivalents needed to synthesis fatty acids.

Role of LXR in transcriptional regulation

A novel transcription factor, RLD-1, was discovered in rats in 1994 (Apfel et al., 1994). This transcription factor was observed to form a heterodimer with RXR and bind to a direct DNA repeat sequence. The human ortholog, named liver-X-receptor-alpha (LXRα), was discovered shortly thereafter (Willy et al., 1995). Two similar proteins, encoded by different genes, with different expression in tissues were identified: LXRα (NR1H3), which is expressed selectively in a few tissues, such as liver and adipose tissue, and LXRβ (NR1H2), which is expressed in all tissues (Song et al., 1994; Seol et al., 1995). Like its rat homolog, LXR binds RXR as a heterodimer. The LXR/RXR heterodimer is capable of being activated either by oxysterols (the LXR ligand) or by 9-cis-retinoic acid (the RXR ligand). Oxysterols capable of activating LXR include 20(S)-hydroxycholesterol, 22(R)-hydroxycholesterol, 24(S),25-epoxycholesterol, 24(S)-hydroxycholesterol, and cholestenoic acid (Forman et al., 1997; Lehmann et al., 1997; Song and Liao, 2000). A detailed survey of oxysterol ligands described the activation of LXRα by a number of oxysterols, but not other sterol compounds such as steroids (Janowski et al., 1996). In general, LXRβ binds similar ligands to LXRα, though there are subtle differences in ligand binding specificity (Janowski et al., 1999). Both LXR proteins are also capable of activation by synthetic agonists such as T0901317 and GW3965 (Mitro et al., Collins et al.)

LXR was shown to be essential in the maintenance of cholesterol and bile acid homeostasis, as LXR knockout mice proved unable to convert excess dietary cholesterol to bile acids for excretion, leading to an excess of hepatic cholesterol (Peet et al., 1998). LXR agonists induced SREBP-1c (but not SREBP-1 or SREBP-2) transcription, and an LXR binding site (LXRE) was identified in the SREBP-1c promoter (Repa et al., 2000). A second LXRE in the SREBP-1c promoter was shortly thereafter identified (Yoshikawa et al., 2001). Inhibition of the cholesterol synthesis pathway by compactin, an inhibitor of HMG-CoA reductase, decreased SREBP-1c transcription in rat hepatoma cells; the decrease was restored by addition of synthetic LXR ligands to culture media, suggesting that endogenous LXR ligands in the cholesterol synthesis pathway are responsible for LXR-mediated SREBP-1c transcription (DeBose-Boyd et al., 2001). The addition of unsaturated fatty acids to the culture medium also inhibited SREBP-1c activation by LXR (Ou et al., 2001).

LXR was also shown to bind to the ChREBP promoter, and induce ChREBP transcription (Cha and Repa, 2007). In addition to its effects on SREBP-1c, LXR directly activates lipoprotein lipase transcription (Zhang et al., 2001), fatty acid synthase (Joseph et al., 2002), and stearoyl-CoA desaturase 1 (Chu et al., 2006), affecting the abundance and character of fatty acid species.

Interrogating gene expression as a marker of ChREBP and SREBP-1 activity

To establish the contributions of SREBP-1c and ChREBP to gene expression, we quantified mRNA levels of genes involved in carbohydrate, lipid, and cholesterol metabolism. Genes that encode enzymes of the lipogenic pathway include acetyl-CoA

synthetase (ACSS2), ATP-citrate lyase (ACLY), Acetyl-CoA carboxylase-1 (ACC1 or ACACA), fatty acid synthase (FASN), long chain fatty-acyl elongase 6 (ELOVL6), and stearoyl-CoA desaturase 1 (SCD1). Acetyl-CoA synthetase, also known as acetate-CoA ligase, uses ATP and acetate to generate acetyl-CoA, pyrophosphate and AMP. ACLY cleaves citrate to generate acetyl-CoA and oxaloacetate. ACC1 carboxylates acetyl-CoA to generate malonyl-CoA, which is acted upon by FASN to add 2-carbon units to the growing fatty acid chain. Similarly to ACC1, acetyl-CoA carboxylase 2 (ACC2, also known as ACACB) generates malonyl-CoA from acetyl-CoA, but ACC2 does this in the mitochondria to regulate fatty acid oxidation. SCD1 desaturates fatty acids such as palmitate and stearate to form the monounsaturated fatty acids palmitoleate and oleate, respectively. Glycerol-3-phosphase acyltransferase (GPAT1) adds fatty acids to glycerol backbones as a step in triglyceride synthesis.

NADP-malic enzyme (hereafter referred to as malic enzyme), glucose-6-phosphate dehydrogenase (G6PD), and 6-phospogluconate dehydrogenase (6PGDH) are all enzymes that reduce $NADP^+$ to NADPH. Malic enzyme oxidizes malate to pyruvate, generating NADPH from $NADP^+$. G6PD and 6PGDH are enzymes in the oxidative phase of the pentose phosphate pathway, which is also called the hexose monophosphate shunt. The pentose phosphate pathway generates NADPH as well as precursors for the synthesis of nucleotides and amino acids. Every two carbons added to a nascent fatty acid chain requires the expenditure of two equivalents of NADPH.

mRNA levels of these lipogenic and NADPH-producing genes are all significantly reduced (to <20%) in refed *L-ChREBP*$^{-/-}$ mice, with the exception of ACSS2, which is

reduced to 40% of control levels. In addition to the lipogenic and NADPH-generating genes, we measured the levels of genes responsible for cholesterol synthesis (HMG-CoA synthase, HMG-CoA reductase, farnesyl diphosphate synthase, and squalene synthase), for the purpose of establishing a control via genes that are not regulated by ChREBP or SREBP-1c. By measuring the changes in gene expression between control and *L-ChREBP*$^{-/-}$ mice, we sought to determine the respective contributions of SREBP-1 and ChREBP to the induction of lipogenic genes in refed mice.

CHAPTER TWO
Results: Part I

GENERATION OF *L-CHREBP*$^{-/-}$ MICE

Location and Rationale for Targeting Cassette

The *L-ChREBP*$^{-/-}$ mouse was developed by using homologous recombination to insert loxP sites upstream of the 9th exon and downstream of the 15th exon of the *ChREBP* gene. When bred to mice expressing a Cre recombinase driven by the albumin promoter, a truncation in the *ChREBP* gene is introduced in only the hepatocytes. Exons 9-15 are removed, leaving exons 1-8 and 16-17 in frame.

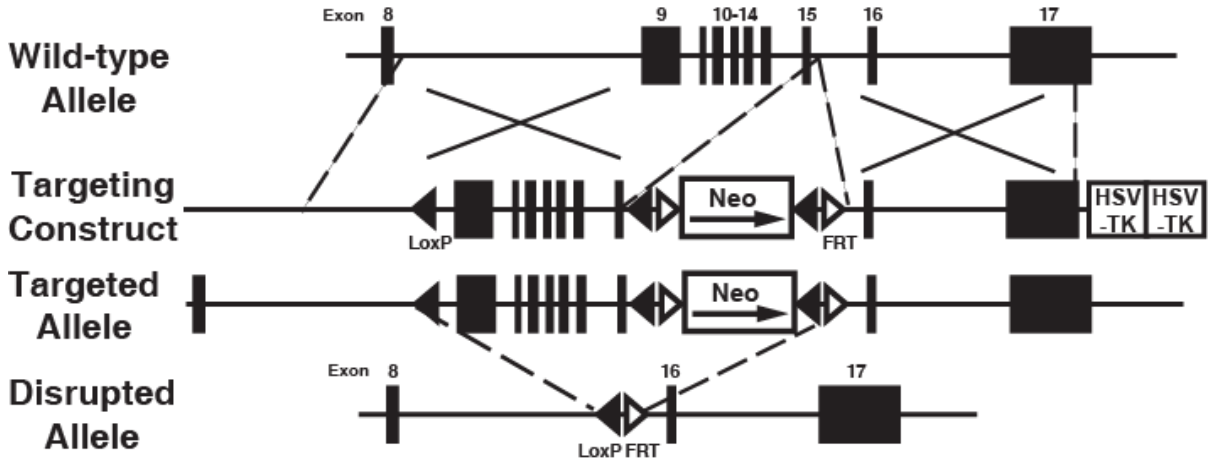

Figure 1: The exons of the wild-type allele are removed via homologous recombination with a targeting construct including loxP sites. In the disrupted allele, exons 9-15 have been removed.

This truncation removes the MLX-interacting domain (proline-rich region) as well as the DNA-binding basic-helix-loop-helix domain of ChREBP. The N-terminal glucose regulatory regions, as well as the ZIP-like region of the extreme C-terminus, remain intact. However, due to the loss of the proline-rich region, which is important for protein-protein

interactions (reviewed in Uyeda and Repa, 2006), and the DNA binding domain, we do not expect the truncated protein to demonstrate any biological activity. A commercially available anti-ChREBP antibody (Novus Biologicals) binds to amino acids 800-852, detecting the truncated ChREBP as well as the full-length protein.

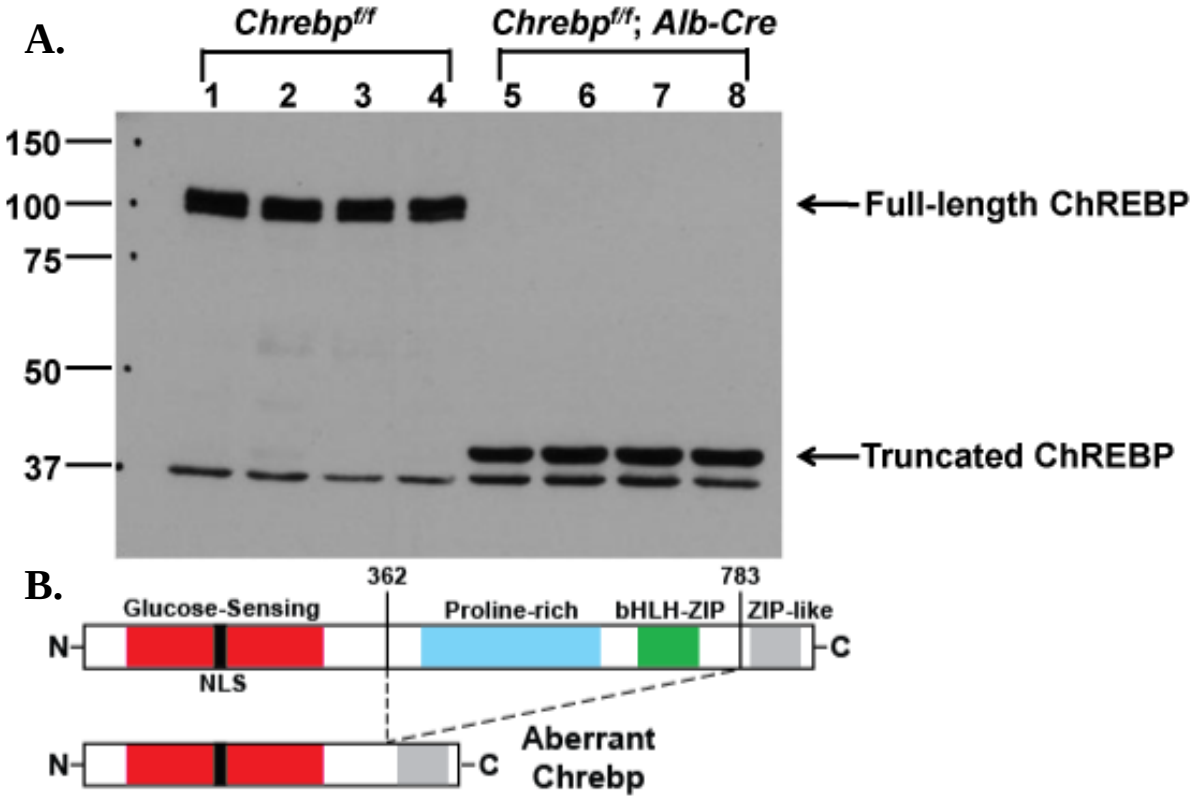

Figure 2: (A) Immunoblot of wild-type (control) and truncated ChREBP protein evident in livers of four *ChREBP*$^{f/f}$ (control) and four *ChREBP*$^{f/f}$, *Alb-Cre*^{tg} (*L-ChREBP*$^{-/-}$) mice. (B) The truncated (aberrant) protein is predicted to consist of 444 amino acids, compared to the 864 amino acids of the full-length protein.

Mice homozygous for the floxed *ChREBP* allele were bred to mice that were homozygous for floxed *ChREBP* as well as heterozygous for an allele expressing Cre recombinase driven by the albumin promoter. All offspring are homozygous for the floxed *ChREBP*, but only 50% of each litter (on average) have Cre recombinase. Mice were

genotyped for Cre recombinase, and sibling cohorts of control (*ChREBP*$^{f/f}$) and *L-ChREBP*$^{-/-}$ (*ChREBP*$^{f/f}$, *Alb-Cre*^{tg}) were used for the studies described in the following sections. Hereafter, *ChREBP*$^{f/f}$, *Alb-Cre*$^{-/-}$ mice, which do not express Cre recombinase, are referred to as control mice for the purposes of the following experiments.

Confirmation of liver-specific deletion

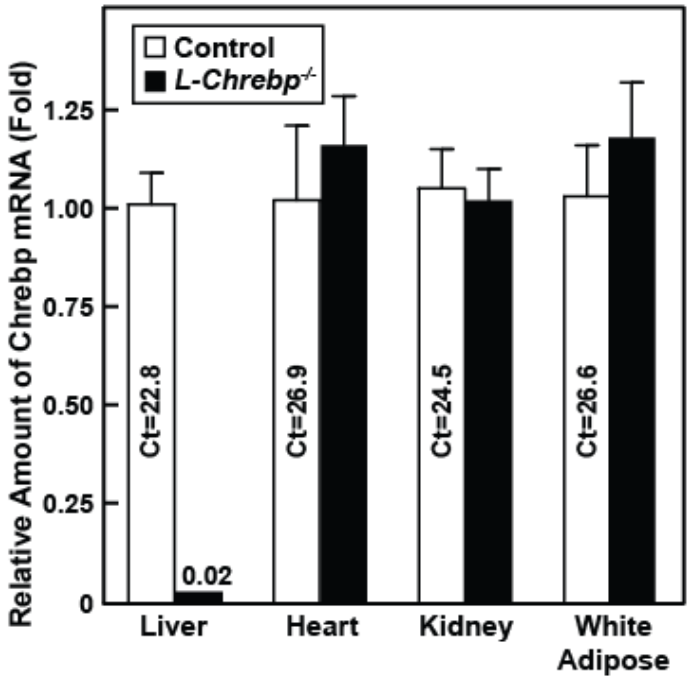

Figure 3: qPCR primers located in the deleted region were used to measure mRNA levels of ChREBP in the liver as well as heart, kidney and white adipose tissue. Full-length ChREBP mRNA was almost completely absent in the liver, while remaining at normal levels in the other tissues measured. Cyclophilin was used as the invariant control. Mean ± SEM of 4 mice is shown.

Having confirmed that the liver-specific deletion was essentially complete via immunoblotting and qPCR, I next set out to characterize the differences between whole-body ChREBP knockout mice and *L-ChREBP*$^{-/-}$ mice.

CHAPTER TWO
Results: Part II

CHARACTERIZATION OF *L-CHREBP*$^{-/-}$ AND *CHREBP*$^{-/-}$ RESPONSE TO HIGH-SUCROSE, ZERO-FAT DIET

Experimental Design

The whole-body ChREBP knockout mouse (hereafter *ChREBP*$^{-/-}$) was previously found to be intolerant to a high-fructose diet (Iizuka et al., 2004). To determine whether *L-ChREBP*$^{-/-}$ mice had the same intolerance, I took control, *ChREBP*$^{-/-}$, and *L-ChREBP*$^{-/-}$ mice that had been maintained on a regular chow diet (44% carbohydrate, 6% fat) and switched them to a high sucrose diet (60% sucrose, 0% fat). (Details of the diets are available in the Methods section.) The experiment consisted of eighteen male mice (ages 7-8 weeks), using six mice of each genotype. Mice were caged individually and their food intake and body mass was measured daily. While both control and *L-ChREBP*$^{-/-}$ mice adapted to the 60% sucrose diet after a few days, *ChREBP*$^{-/-}$ mice persistently ate less than half their usual food intake (Figure 4).

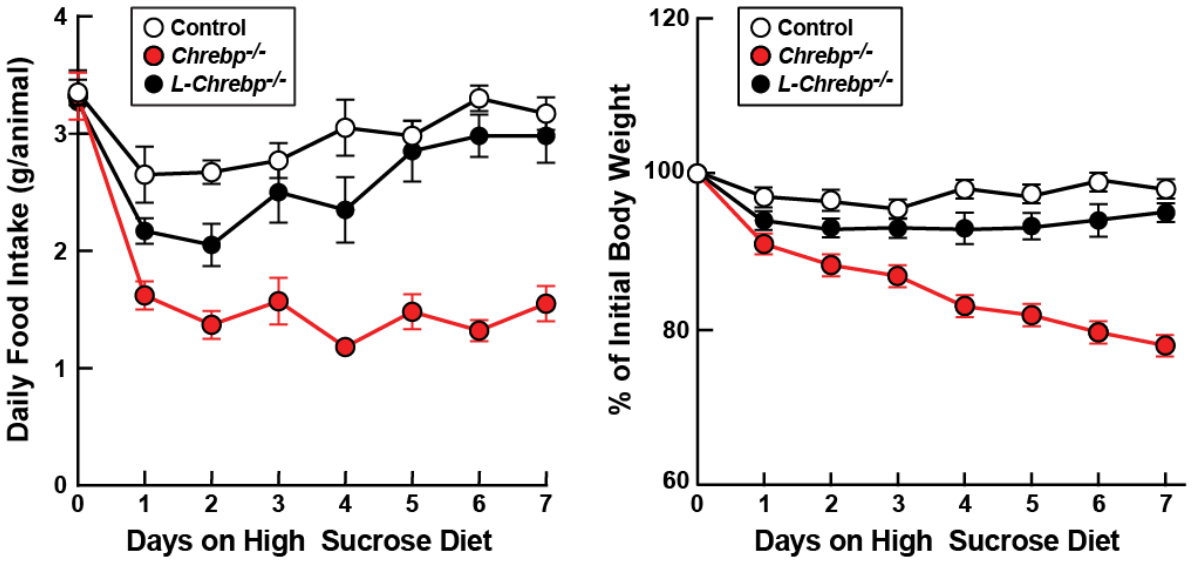

Figure 4: Comparison of control, *ChREBP*$^{-/-}$, and *L-ChREBP*$^{-/-}$ mice that were switched to 60% sucrose, 0% fat diet on day 0. Control and *L-ChREBP*$^{-/-}$ mice regained their feeding behavior after a few days, but *ChREBP*$^{-/-}$ mice were unable to adapt to the diet. Mean ± SEM of 6 mice is shown.

Control mice maintained their body mass over the course of 7 days of high-sucrose diet feeding. *L-ChREBP*$^{-/-}$ mice lost 5% of body mass over 7 days, while *ChREBP*$^{-/-}$ mice lost 21% of their body mass. Over days 5-7, control mice ate an average of 3.2 grams of food per day (98% of previous chow diet intake), while *L-ChREBP*$^{-/-}$ mice ate 2.9 grams (92% of previous chow intake) and *ChREBP*$^{-/-}$ mice ate 1.5 grams (45% of previous chow intake). *L-ChREBP*$^{-/-}$ mice thus tolerate a high-sucrose diet, allowing fasting-refeeding with this diet.

CHAPTER TWO
Results: Part III

CHARACTERIZATION OF *L-CHREBP*$^{-/-}$ PHENOTYPE

Experimental Design

Having established that *L-ChREBP*$^{-/-}$ mice tolerated a high-sucrose, fat-free diet, my next objective was to characterize the metabolic phenotype associated with the liver-specific ChREBP knockout mouse. It seemed likely that the *L-ChREBP*$^{-/-}$ mouse would share some phenotypic characteristics with the whole-body ChREBP knockout mouse as previously characterized (Iizuka et al., 2004). Thus, I sought to measure mRNA levels of known ChREBP target genes, as well as conduct metabolic assays of glucose and fatty acid metabolites in the liver and plasma.

Twelve control and twelve *L-ChREBP*$^{-/-}$ mice were divided into three groups of mice per genotype (n = 4 per group) and their access to food was altered. One group of mice of each genotype was allowed ad libitum access to food, another group per genotype of mice were fasted for 12 hours prior to tissue collection, and a third group per genotype was fasted 12 hours, then allowed access to food for 12 hours prior to tissue collection. The detailed nonfasting/fasting/refeeding protocol is described in the Methods section. Tissues were harvested from all mice at 9 AM at the beginning of the light cycle. Blood glucose was measured from the tail vein, then the mice were anesthetized and whole blood and liver tissue was collected. Blood was centrifuged in EDTA-coated tubes to isolate plasma, while the livers were frozen in liquid nitrogen for later analysis of mRNA and metabolite levels.

Detailed procedures for mouse housing and tissue collection are described in the Methods section.

Plasma insulin levels in control and *L-ChREBP*$^{-/-}$ mice

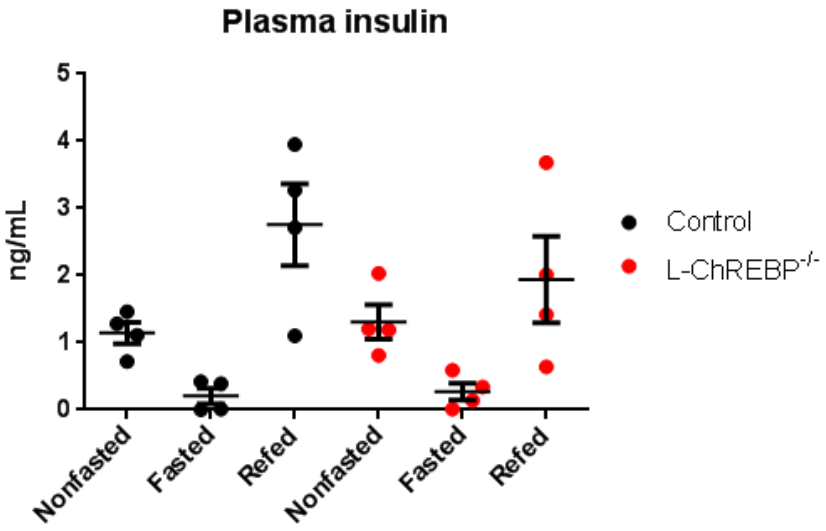

Figure 5: Plasma insulin in control and *L-ChREBP*$^{-/-}$ mice.
Mean ± SEM is plotted, n=4 per group.

Plasma insulin in both control and *L-ChREBP*$^{-/-}$ mice was increased in the refed state and decreased in the fasted state relative to the nonfasted values (Figure 5 and Table 2). Statistical tests (two-tailed Student's *t*-test) showed that insulin levels of the two mouse genotypes in a given feeding status were not significantly different. Thus, the differences in gene expression and fatty acid metabolism between the two genotypes are likely not due to differences in insulin levels.

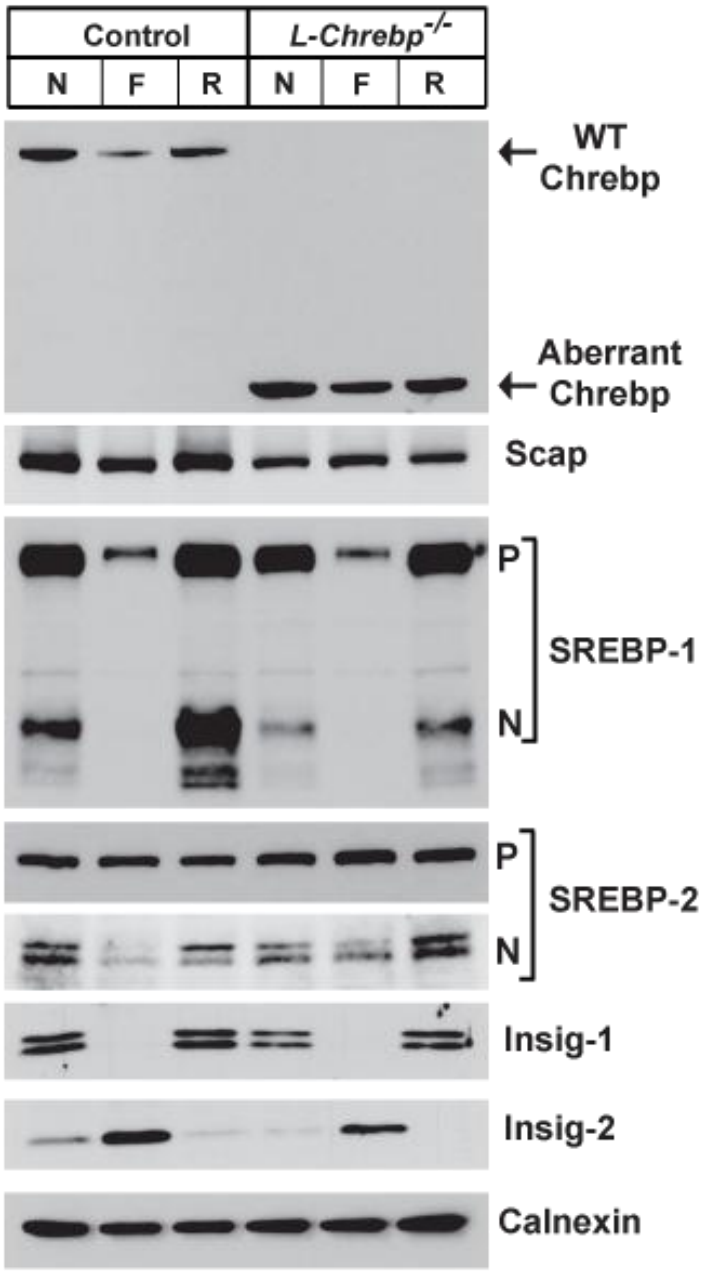

Figure 6: Protein immunoblots of ChREBP, SCAP, SREBP-1, SREBP-2, Insig-1, Insig-2 and GAPDH in whole cell extracts derived from livers of control and *L-ChREBP*$^{-/-}$ mice. Protein was normalized to 30 µg per lane via BCA assay. Extracts from 4 mice are pooled in each lane. Calnexin was used as the loading control.

Regulatory protein abundance

The expression of various proteins was measured by immunoblotting of whole cell lysate derived from liver extracts. Detailed procedures for tissue processing and immunoblotting are described in the Methods section. Control ChREBP was detected as a band at approximately 95 kDa, while truncated ChREBP protein was visible around 40 kDa in the *L-ChREBP*$^{-/-}$ mice. ChREBP was increased in the nonfasted and refed states relative to the fasted condition.

Scap expression was relatively constant irrespective of feeding status in control and *L-ChREBP*$^{-/-}$ mice. SREBP-1,

of which the primary isoform is SREBP-1c in the liver, is transcriptionally upregulated by insulin, and correspondingly precursor (P) SREBP-1 was increased in the nonfasted and refed states of both genotypes of mice. The processing of SREBP-1 is even more strongly dependent upon refeeding; however, the refed *L-ChREBP*$^{-/-}$ mice only contained 45% of the nuclear SREBP-1 (N) present in refed control mice, and nonfasted *L-ChREBP*$^{-/-}$ mice only contained 63% of the nuclear SREBP-1 present in control mice. While ChREBP has no known direct role in regulating SREBP-1 transport to the Golgi or its proteolytic cleavage, it is possible that a ChREBP target gene affects SREBP-1 processing.

Nuclear SREBP-2 processing was readily detected in the nonfasted and refed groups of both genotypes. As expected, Insig-1 was decreased in the fasted condition, while Insig-2 was increased in the fasted condition. The abundance of both Insig proteins did not differ between the mice of the two genotypes. Levels of calnexin, an ER membrane protein, were used as the loading control.

Alterations in mRNA levels of *L-ChREBP*$^{-/-}$ mice

Table 1 shows the mRNA levels of various selected genes in the livers of control and *L-ChREBP*$^{-/-}$ mice according to feeding condition. All mRNA levels were normalized using the mRNA level of ApoB present in each group, and are stated as a multiple of the mRNA level of that particular gene measured in fasted control mice. ChREBP target genes such as pyruvate kinase and RGS16 were dramatically decreased in the *L-ChREBP*$^{-/-}$ mouse. Of particular note are the enzymes directly responsible for fatty acid synthesis and the generation of malonyl-CoA and NADPH. All genes in the lipogenic pathway were decreased

by 80-97% in the *L-ChREBP*$^{-/-}$ mouse relative to the control mouse, except for ACSS2, which was decreased by only 62%. NADPH-generating genes were decreased by 70-90%. Graphical illustrations of particular gene pathways are shown in Figures 7-9.

Table 1

Relative amounts of mRNAs in livers of control and *L-ChREBP*$^{-/-}$ mice subjected to fasting and refeeding

mRNAs	Control			*L-ChREBP*$^{-/-}$		
	N	F	R	N	F	R
ApoB (Ct)	1.00 (18.2)	1.00 (17.7)	1.00 (18.1)	1.00 (18.0)	1.00 (17.6)	1.00 (18.0)
ChREBP and glucose metabolism						
ChREBP-total, truncated region	4.05	1.00 (23.9)	6.11	0.02	0.01	0.01
ChREBP-α	2.76	1.00 (22.0)	2.58	1.41	0.43	0.99
ChREBP-β	2.29	1.00 (24.9)	14.19	0.08	0.02	0.04
L-Pyruvate Kinase	5.73	1.00 (22.3)	22.37	0.75	0.17	0.56
Glut-2	2.31	1.00 (28.0)	2.13	0.51	0.24	0.17
Glucokinase	14.6	1.00 (29.2)	22.38	20.61	2.81	27.41
Fructokinase	2.82	1.00 (22.6)	6.13	1.44	0.50	1.10
Triose kinase	1.87	1.00 (22.4)	8.12	0.74	0.28	0.90
PEPCK	0.54	1.00 (18.4)	0.15	0.56	1.10	0.35
G6PC	0.94	1.00 (19.7)	1.90	0.47	0.69	0.60
RGS16	0.31	1.00 (23.9)	2.05	0.05	0.05	0.02
SREBP pathway						
Scap	1.73	1.00 (24.4)	2.73	1.44	1.04	1.32
SREBP-1a	0.80	1.00 (26.0)	1.61	0.69	1.15	0.83
SREBP-1c	33.08	1.00 (26.3)	68.91	32.92	0.65	35.82
SREBP-2	2.05	1.00 (23.9)	2.09	2.63	1.74	2.93
Insig-1	7.28	1.00 (23.9)	12.15	6.78	2.10	9.12
Insig-2-total	0.79	1.00 (20.6)	0.85	0.66	1.20	0.64
Insig-2a	0.81	1.00 (22.3)	0.88	0.62	1.29	0.64
Insig-2b	1.49	1.00 (25.6)	1.23	2.17	1.40	1.80
Fatty acid and triglyceride synthesis						
ATP citrate lyase	8.07	1.00 (23.5)	59.31	3.85	0.80	6.03
Acetyl-CoA synthetase	8.74	1.00 (24.6)	22.07	5.79	1.09	8.41
Acetyl-CoA carboxylase 1	4.26	1.00 (24.9)	24.55	2.93	0.79	2.64
Acetyl-CoA carboxylase 2	2.46	1.00 (23.8)	6.50	0.58	0.83	0.77
Fatty acid synthase	14.8	1.00 (23.3)	83.18	4.69	0.70	6.06
Long chain fatty acyl elongase 6	4.62	1.00 (24.9)	61.02	1.47	0.28	1.85
Stearoyl-CoA desaturase-1	4.39	1.00 (18.4)	6.22	1.47	0.27	0.60
Glycerol-3-phosphate acyltransferase	2.10	1.00 (22.3)	9.34	1.41	1.42	1.49
Malic enzyme	2.29	1.00 (21.8)	10.48	0.33	0.36	0.32
glucose-6-phosphate dehydrogenase	2.42	1.00 (27.9)	8.92	2.14	1.43	1.69
6-phosphogluconate dehydrogenase	2.70	1.00 (25.1)	13.5	1.94	1.00	2.31
Cholesterol synthesis and uptake						
HMG-CoA synthase	4.92	1.00 (22.8)	9.20	4.87	2.08	8.95
HMG-CoA reductase	6.39	1.00 (25.6)	11.90	5.20	1.49	7.64
FDP synthase	14.15	1.00 (25.5)	36.63	13.61	2.22	22.18
Squalene synthase	5.01	1.00 (23.2)	7.47	5.69	1.73	9.64
LDL receptor	2.86	1.00 (24.0)	4.84	2.96	1.45	4.03
PCSK9	18.26	1.00 (29.0)	29.90	18.76	1.78	27.22
LXR targets						
LXRa	1.38	1.00 (23.7)	1.40	1.62	1.13	1.87
LXRb	1.28	1.00 (28.3)	1.30	1.43	1.35	1.65
ABCA1	1.82	1.00 (23.4)	2.28	1.92	1.17	1.57
ABCG5	1.42	1.00 (25.3)	0.88	1.56	0.89	0.78
ABCG8	1.18	1.00 (23.7)	0.65	1.14	0.85	0.53

The mice used here are the same as those described in Table 2. For each group, equal amounts of total RNA from 4 mice were pooled and subjected to real-time PCR quantification. ApoB was used as the invariant control. Values represent the amount of mRNA relative to that in fasted control mice, which is arbitrarily defined as 1. The Ct number of each gene in fasted control mice was noted in the parenthesis.

mRNA induction of lipogenic genes in refed mice

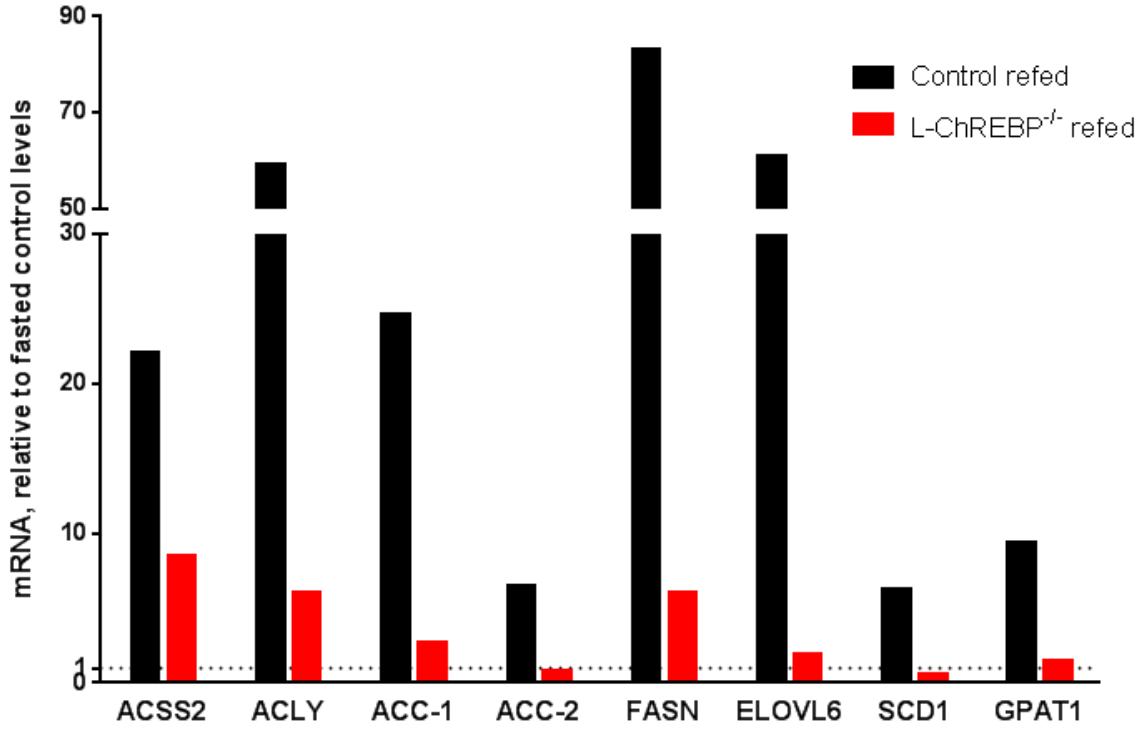

Figure 7: mRNA levels of lipogenic genes in refed control and *L-ChREBP*$^{-/-}$ mice

Figure 7 shows mRNA levels of the genes responsible for lipogenesis in control and *L-ChREBP*$^{-/-}$ refed mice. ACSS2 and ACLY, two genes responsible for the generation of Acetyl-CoA, show mRNA levels decreased by 62% in ACSS2 and 90% in ACLY. ACC1, responsible for the generation of malonyl-CoA, was decreased by 89%, while ACC2, which inhibits the oxidation of fatty acids in the mitochondria, was decreased by 88%. Fatty acid synthase, which generates palmitic acid from malonyl-CoA, was decreased by 93%, and long chain elongase, which extend palmitic acid by two carbons to form stearic acid, was decreased by 97%. SCD1, which desaturates stearate to oleate, was decreased by 90%, and GPAT1, which attaches fatty acids to glycerol-3-phosphate to begin building triglycerides,

was decreased by 84%. Clearly, ChREBP is required for the carbohydrate-stimulated induction of lipogenic genes.

In addition to genes responsible for lipogenesis, we measured the mRNAs for the enzymes responsible for the generation of NADPH, which is a necessary cofactor in lipogenesis. The mRNA levels of NADPH-generating genes are shown in Figure 8.

mRNA induction of NADPH-producing genes in refed mice

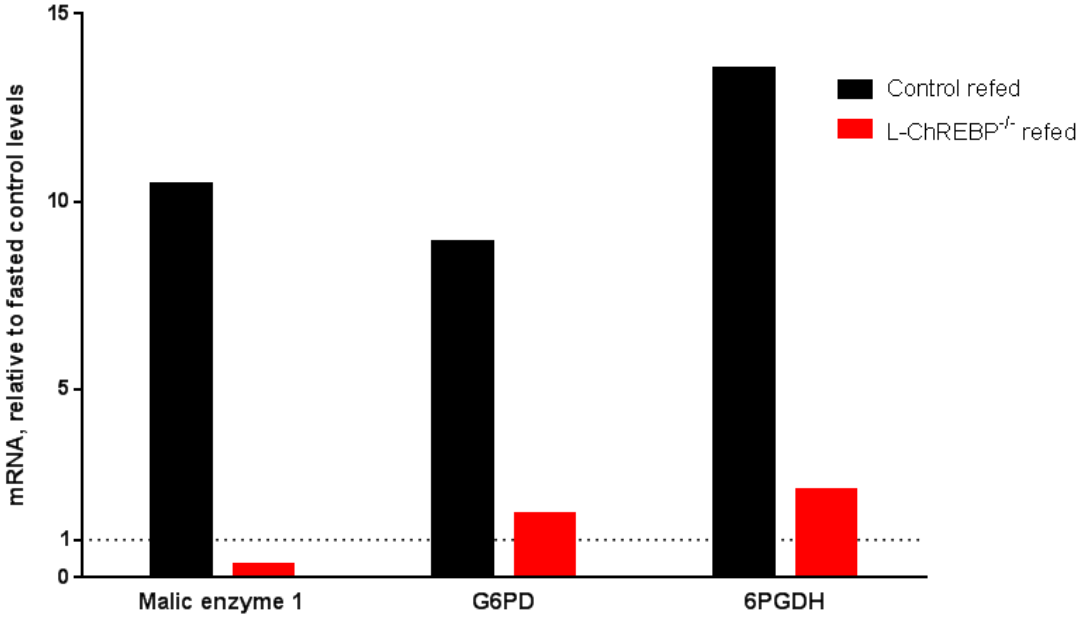

Figure 8: mRNA levels of NADPH-producing genes in control and *L-ChREBP*$^{-/-}$ mice

mRNAs for NADPH-generating enzymes in *L-ChREBP*$^{-/-}$ mice were decreased by 97% for malic enzyme, 81% for glucose-6-phosphate dehydrogenase, and 83% for 6-phosphogluconate dehydrogenase, respectively. Since NADPH is an essential cofactor for lipogenesis, it is not surprising that ChREBP plays a part in its regulation, as it does the lipogenic enzymes. However, not all lipid-biosynthetic pathways were affected by ChREBP disruption. An example of a gene pathway that ChREBP deletion does not uniformly

decrease is the cholesterologenic pathway. Figure 9 shows the mRNA levels of sterologenic genes in control and *L-ChREBP*$^{-/-}$ mice.

mRNA induction of cholesterol-producing genes in refed mice

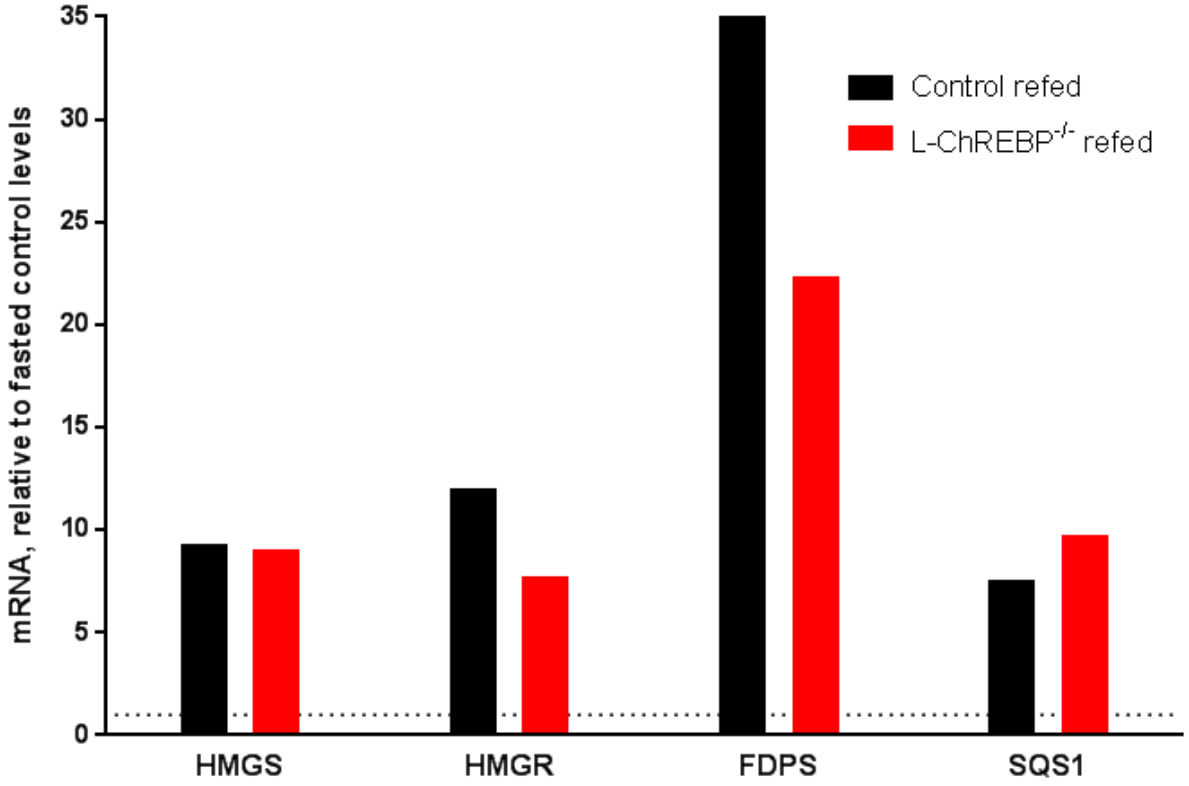

Figure 9: mRNA levels of cholesterol-producing genes in control and *L-ChREBP*$^{-/-}$ mice

While there was a 35% decrease in HMG-CoA reductase and a 39% decrease in farnesyl diphosphate synthase, there was a 29% increase in squalene synthase and a negligible change in HMG-CoA synthase. The sterologenic genes did not show a generalized pattern of loss of refeeding induction in *L-ChREBP*$^{-/-}$ mice, as was observed in the lipogenic genes. Rather than being governed by ChREBP or SREBP-1, the sterologenic genes are primarily regulated by SREBP-2.

Table 2

Effects of fasting and refeeding on control and *L-ChREBP*$^{-/-}$ mice

	Control			*L-ChREBP*$^{-/-}$		
Parameter	**Nonfasted**	**Fasted**	**Refed**	**Nonfasted**	**Fasted**	**Refed**
Number of mice	4	4	4	4	4	4
Body weight (g)	34.8 ± 1.0	30.6 ± 1.3	37.5 ± 1.8	38.4 ± 0.2*	30.6 ± 1.0	35.2 ± 1.5
Liver weight (g)	1.5 ± 0.06	1.3 ± 0.06	1.9 ± 0.08	2.0 ± 0.1**	1.3 ± 0.06	2.2 ± 0.15
Liver weight/body weight (%)	4.3 ± 0.1	4.1 ± 0.2	5.0 ± 0.1	5.2 ± 0.3*	4.4 ± 0.1	6.1 ± 0.3**
Liver cholesterol content (mg/g)	1.93 ± 0.07	2.34 ± 0.27	1.87 ± 0.08	1.67 ± 0.06*	2.82 ± 0.23	1.53 ± 0.07*
Liver triglyceride content (mg/g)	19 ± 3	95 ± 8	35 ± 5	52 ± 3**	167 ± 15**	43 ± 5
Liver glycogen content (mg/g)	46 ± 9	1.8 ± 0.8	101 ± 7	79 ± 9*	2.3 ± 1.0	122 ± 5
Total plasma cholesterol (mg/dL)	156 ± 11	129 ± 10	128 ± 4	118 ± 1*	87 ± 2**	81 ± 2**
Total plasma triglyceride (mg/dL)	190 ± 9	178 ± 9	164 ± 16	232 ± 23	170 ± 13	172 ± 13
Plasma aspartate transaminase (U/L)	41 ± 5	55 ± 13	40 ± 3	52 ± 1	44 ± 11	43 ± 3
Plasma alanine transaminase (U/L)	41 ± 2	48 ± 2	36 ± 3	65 ± 2**	70 ± 6*	59 ± 5**
Plasma insulin (ng/mL)	1.1 ± 0.02	0.29 ± 0.09	2.8 ± 0.6	1.3 ± 0.3	0.19 ± 0.14	1.9 ± 0.7
Plasma glucose (mg/dL)	264 ± 10	156 ± 25	231 ± 13	227 ± 5*	125 ± 13	190 ± 12

Control (*ChREBP*$^{f/f}$) and *L-ChREBP*$^{-/-}$ (*ChREBP*$^{f/f}$*;Alb-Cre*) littermates (male, 7 months of age) were subjected to fasting and refeeding. The nonfasted group was maintained on ad libitum chow diet, the fasted group was fasted 12 h, and the refed group was fasted for 12 h and then refed a high-carbohydrate/fat-free diet for 12 h prior to study. The starting times for the feeding regimens were staggered so that all mice were sacrificed at the same time, which was at the end of the dark cycle. Each value represents the mean ± SEM. Asterisks denote the level of statistical significance between control and *L-ChREBP*$^{-/-}$ mice of the same dietary treatment. *P<0.05 and **P<0.01.

Analysis of blood plasma metabolites

Plasma cholesterol levels were decreased in the fasted and refed conditions compared to the nonfasted condition for both genotypes. Plasma cholesterol levels were decreased in all *L-ChREBP*$^{-/-}$ groups compared to their respective control groups: 25% in nonfasted mice, 33% in fasted mice, and 37% in refed mice. Plasma triglycerides were similar across all genotypes and feeding conditions. This is consistent with previous results from the whole-body ChREBP knockout mouse (Iizuka et al., 2004).

Alanine aminotransferase levels were increased in *L-ChREBP*$^{-/-}$ mice under all feeding conditions. The increases were 57% in nonfasted mice, 45% in fasted mice, and 63% in refed mice. Aspartate aminotransferase levels were not significantly different between the two genotypes, nor did they vary based on feeding conditions. Plasma glucose was decreased by 14% in the *L-ChREBP*$^{-/-}$ nonfasted mice relative to control nonfasted mice. No statistically significant differences in plasma glucose were observed between the two genotypes in the fasted or refed conditions.

Analysis of liver triglycerides, cholesterol, and glycogen

Liver cholesterol levels were decreased 13% in nonfasted *L-ChREBP*$^{-/-}$ mice compared to nonfasted control mice and by 18% in refed *L-ChREBP*$^{-/-}$ mice compared to refed control mice. Fasted mice did not show any significant change in liver cholesterol levels. Liver triglycerides in *L-ChREBP*$^{-/-}$ mice were increased by 171% in the nonfasted state and by 76% in the fasted state, but no difference was observed in the refed state between the two genotypes. Liver glycogen was increased by 80% in nonfasted *L-ChREBP*$^{-/-}$ mice compared to nonfasted control mice, but other feeding conditions showed no significant change in liver glycogen between the two genotypes.

CHAPTER TWO
Results: Part IV

RESTORATION OF SREBP-1C IN *L-CHREBP*$^{-/-}$ MICE

Experimental Design

The previous experiment established that the *L-ChREBP*$^{-/-}$ mouse exhibited greatly diminished mRNA levels of lipogenic genes upon refeeding. However, the approximately 75% decrease in nuclear SREBP-1 protein in refed *L-ChREBP*$^{-/-}$ mice relative to control mice introduced a major confounding factor that prevented the determination of whether the fall in transcription of lipogenic genes resulted from the absence of ChREBP or from the resulting decrease in nuclear SREBP-1. To restore nuclear SREBP-1c, I cloned the N-terminal 456 amino acids of mouse SREBP-1c into an adeno-associated virus. This 456-residue protein is identical to SREBP-1c after its proteolytic processing by S1P and S2P. The AAV-DJ serotype is essentially specific to the liver and requires 1-2 weeks to reach peak gene expression. We utilized another AAV-DJ adeno-associated virus expressing GFP to serve as a control virus.

Control mice were injected with AAV-DJ-GFP and divided into a fasted group and a refed group. *L-ChREBP*$^{-/-}$ mice were injected with either AAV-DJ-GFP (two groups, one fasted and one refed) or AAV-DJ-SREBP-1c (one refed group). Seven days after viral injection, mice were subjected to the fasting or refeeding protocols as appropriate (see Methods section). At 9 AM on the eighth day after viral injection, all mice were sacrificed.

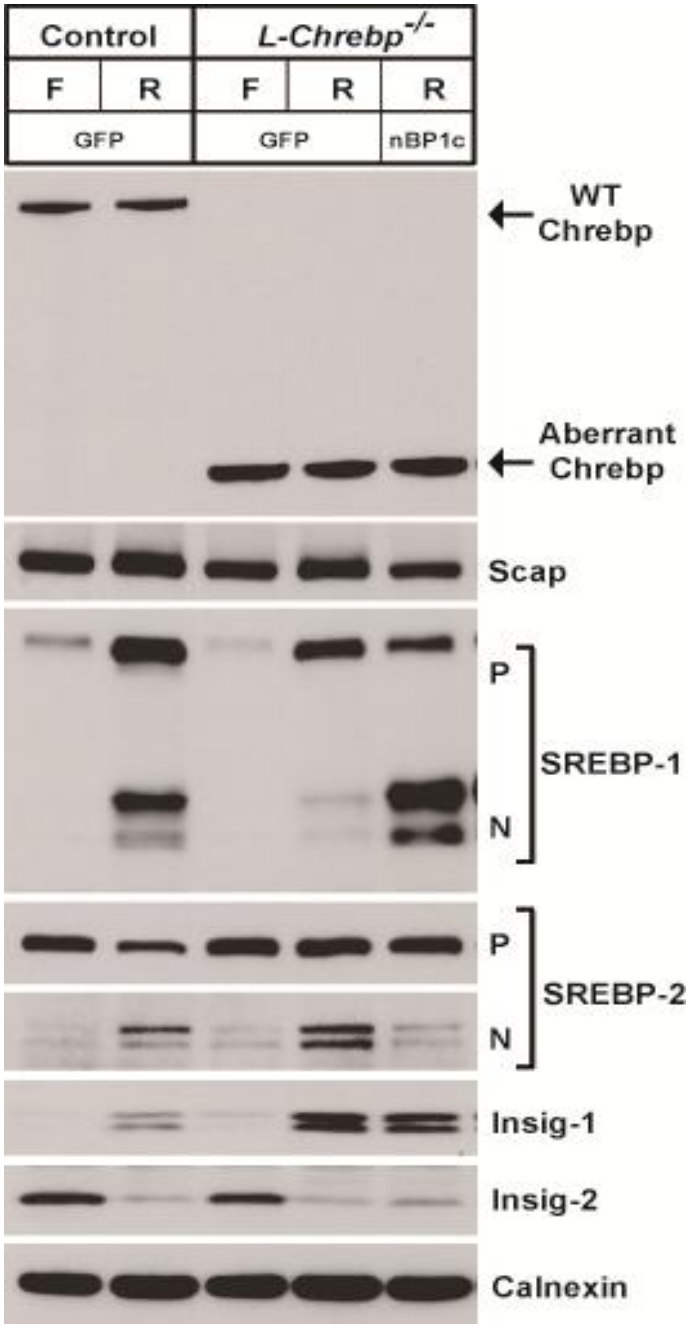

Figure 10: Protein immunoblots of ChREBP, SCAP, SREBP-1, SREBP-2, Insig-1, and Insig-2 in whole cell extract derived from livers of AAV-injected control and *L-ChREBP*$^{-/-}$ mice. 30 µg total protein, determined via BCA assay, was pooled from 4-6 mice per group. Calnexin was used as the loading control.

Blood glucose was measured, mice were anesthetized, and finally blood and liver tissue was harvested as in the previous experiment.

Regulatory protein abundance

Full-length ChREBP was only detectable in both groups of control mice, while only the truncated form of ChREBP was detected in the *L-ChREBP*$^{-/-}$ mice, as expected. Scap remains largely constant among all groups of mice. Insig-1 was present in all refed groups, as expected, and was increased in refed *L-ChREBP*$^{-/-}$ mice compared to refed control mice. Insig-2 was present at high levels in fasted groups of mice, and at low levels in refed groups, as was observed previously.

The unprocessed SREBP-1 precursor protein (P) was present at

high levels in refed mice and at low levels in fasted mice. Levels of precursor SREBP-1 protein were decreased in *L-ChREBP*$^{-/-}$ mice relative to control refed mice. However, a much more striking difference was seen in the levels of processed, nuclear SREBP-1 (N). Normally, refeeding mice stimulates the processing of SREBP-1, as seen in control refed mice. However, the *L-ChREBP*$^{-/-}$ mice failed to process SREBP-1 effectively, and refed *L-ChREBP*$^{-/-}$ AAV-GFP-injected mice exhibited minimal levels of processed SREBP-1. Injection of AAV- SREBP-1c restored nuclear SREBP-1 to levels to similar to those in control mice.

SREBP-2 precursor (P) levels were largely unchanged among the groups, while processed SREBP-2 was highest in the refed groups. Calnexin was used as a loading control.

Plasma insulin levels

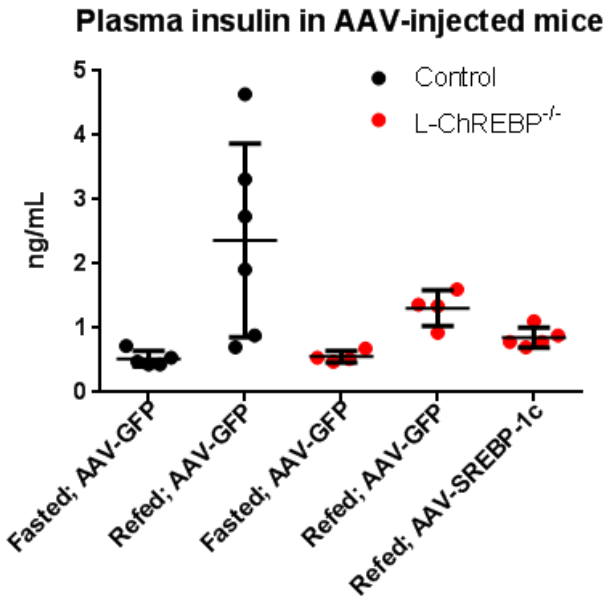

Figure 11: Plasma insulin in AAV-injected control and *L-ChREBP*$^{-/-}$ mice

Control refed mice demonstrated a wide variation in insulin levels, while fasted mice of both genotypes and refed *L-ChREBP*$^{-/-}$ mice exhibited tightly consistent insulin values. However, there was no statistically significant difference between the control refed animals and *L-ChREBP*$^{-/-}$ refed mice (Student's *t*-test).

Plasma glucose levels

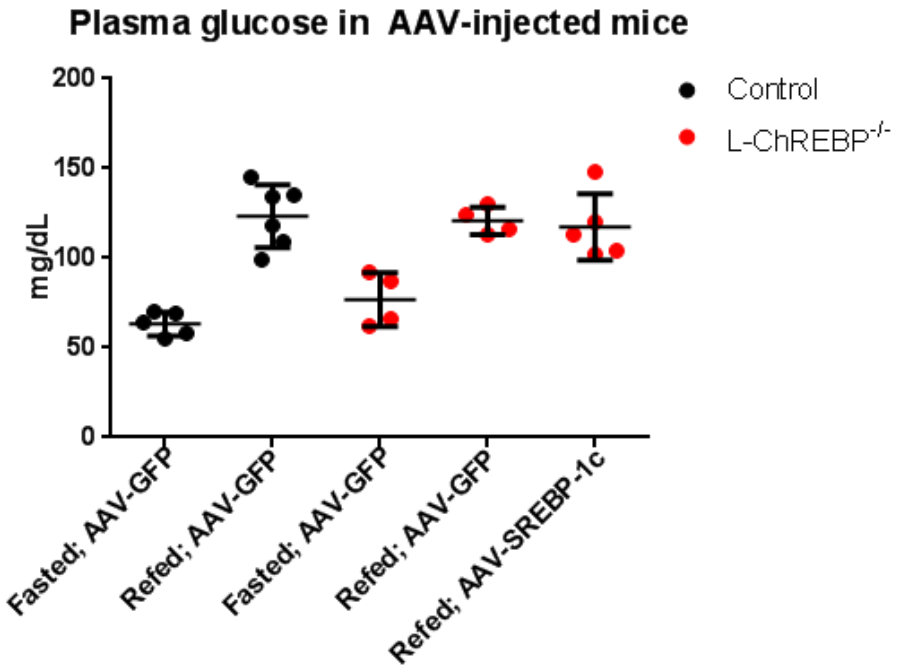

Figure 12: Plasma glucose in AAV-injected control and *L-ChREBP*$^{-/-}$ mice

Blood glucose levels were increased in the refed state of both genotypes and regardless of whether the mice were injected with GFP or SREBP-1c AAV. Values are presented in Table 4. There were no significant differences based on either genotype or type of virus injected.

Alterations in mRNA levels based on genotype and type of virus injected

Table 3 gives measured mRNA levels for all measured genes. As shown by the immunoblots above, AAV-SREBP-1c injection restored nuclear SREBP-1 in refed *L-ChREBP*$^{-/-}$ mice to levels similar to those present in refed control AAV-GFP injected mice. Additionally, LXR levels were not decreased in *L-ChREBP*$^{-/-}$ mice. Thus, the response of lipogenic genes in the AAV-SREBP-1c injected mice can be used to determine whether their reduced expression in *L-ChREBP*$^{-/-}$ mice is solely due to the reduction in nuclear SREBP-1c present in *L-ChREBP*$^{-/-}$ mice.

Table 3

Relative amounts of mRNAs in livers of AAV-injected control and *L-ChREBP*$^{-/-}$ mice subjected to fasting and refeeding

	Control		*L-ChREBP*$^{-/-}$		
	F	**R**	**F**	**R**	**R**
AAV injected	GFP	GFP	GFP	GFP	SREBP-1c
mRNAs					
ApoB (Ct)	1.00 (18.6)	1.00 (18.6)	1.00 (18.8)	1.00 (18.4)	1.00 (18.6)
ChREBP and glucose metabolism					
ChREBP-total, truncated region	1.00 (25.4)	6.46	0.01	0.02	0.03
ChREBP-α	1.00 (22.9)	3.14	0.54	1.04	1.38
ChREBP-β	1.00 (26.1)	16.37	0.04	0.13	0.27
L-Pyruvate Kinase	1.00 (23.6)	23.29	0.24	0.78	1.03
Glut-2	1.00 (29.3)	2.17	0.29	0.26	0.49
Glucokinase	1.00 (30.8)	38.63	3.14	75.08	69.68
Fructokinase	1.00 (23.7)	6.59	0.53	1.06	1.10
Triose kinase	1.00 (23.4)	9.55	0.32	0.92	0.72
PEPCK	1.00 (19.8)	0.18	1.16	0.38	0.65
G6PC	1.00 (21.0)	2.81	0.61	0.64	0.77
RGS16	1.00 (27.2)	15.10	0.30	0.62	1.21
SREBP pathway					
Scap	1.00 (26.3)	2.89	1.08	1.81	2.69
SREBP-1a	1.00 (26.9)	4.48	1.05	3.36	3.17
SREBP-1c	1.00 (28.6)	81.58	1.33	35.16	41.58
SREBP-2	1.00 (25.0)	3.20	1.71	4.78	4.40
Insig-1	1.00 (26.1)	30.86	2.71	29.85	38.83
Insig-2-total	1.00 (21.6)	0.60	0.97	0.52	0.67
Insig-2a	1.00 (24.0)	0.73	1.02	0.64	0.86
Insig-2b	1.00 (27.7)	1.81	1.36	2.54	2.78
Fatty acid and triglyceride synthesis					
ATP citrate lyase	1.00 (25.0)	98.82	1.02	13.45	38.37
Acetyl-CoA synthetase	1.00 (25.4)	18.02	1.10	12.62	22.90
Acetyl-CoA carboxylase 1	1.00 (26.0)	25.27	0.94	3.66	4.79
Acetyl-CoA carboxylase 2	1.00 (24.6)	5.03	0.80	0.92	4.87
Fatty acid synthase	1.00 (24.0)	84.72	0.65	10.50	14.43
Long chain fatty acyl elongase 6	1.00 (25.6)	42.18	0.30	2.14	3.29
Stearoyl-CoA desaturase-1	1.00 (19.4)	4.29	0.36	0.63	3.07
Glycerol-3-phosphate acyltransferase	1.00 (23.2)	12.49	1.27	2.60	6.90
Malic enzyme	1.00 (22.9)	13.00	0.35	0.75	2.66
glucose-6-phosphate dehydrogenase	1.00 (28.6)	9.34	1.37	2.09	22.89
6-phosphogluconate dehydrogenase	1.00 (26.2)	16.26	0.97	3.67	5.23
Cholesterol synthesis and uptake					
HMG-CoA synthase	1.00 (24.1)	13.75	1.68	25.11	14.93
HMG-CoA reductase	1.00 (26.9)	16.51	1.77	22.08	20.14
FDP synthase	1.00 (26.2)	41.42	1.43	40.64	36.71
Squalene synthase	1.00 (24.7)	12.21	2.08	25.90	14.28
LDL receptor	1.00 (24.9)	5.14	1.50	4.75	5.56
PCSK9	1.00 (30.1)	35.17	2.25	37.95	29.96
LXR targets					
LXRa	1.00 (25.7)	1.89	1.25	2.27	2.42
LXRb	1.00 (29.9)	1.29	1.17	1.63	1.99
ABCA1	1.00 (25.4)	2.06	1.09	1.55	1.45
ABCG5	1.00 (27.1)	0.85	1.25	1.11	1.36
ABCG8	1.00 (25.9)	0.66	1.29	0.93	1.25

The mice used here are the same as those described in Table 4. For each group, equal amounts of total RNA from all mice in the group were pooled and subjected to real-time PCR quantification. ApoB was used as the invariant control. Values represent the amount of mRNA relative to that in fasted control mice, which is arbitrarily defined as 1. The Ct number of each gene in fasted control mice was noted in the parenthesis.

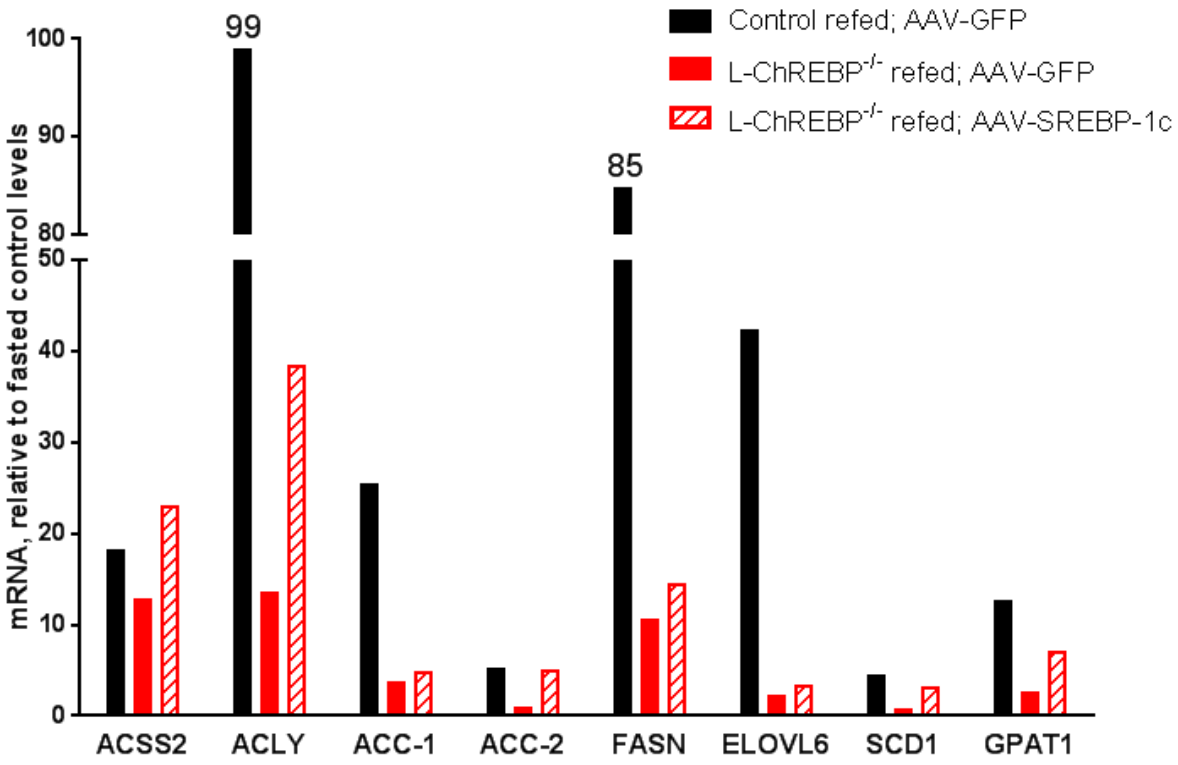

mRNA induction of lipogenic genes in refed, AAV-injected mice

Figure 13: mRNA induction of lipogenic genes in AAV-GFP control mice, AAV-GFP *L-ChREBP*$^{-/-}$ mice, and AAV-SREBP-1c *L-ChREBP*$^{-/-}$ mice.

In the absence of SREBP-1c virus, all lipogenic and NADPH-generating genes were decreased more than 80%, with the exception of ACSS2. With AAV-SREBP-1c, some genes were fully restored or overexpressed, some genes were partially restored, and some genes were largely unaffected by the virus.

A number of genes failed to significantly increase in the refed *L-ChREBP*$^{-/-}$ mice injected with AAV-SREBP-1c relative to those that received AAV-GFP. Fatty acid synthase and ACC1, the two core genes of lipogenesis, were decreased by more than 80% after SREBP-1 restoration, relative to refed control mice (Figure 13). Long chain elongase,

immediately downstream of FASN, remained reduced by 92% (Figure 13). The NADPH-generating genes malic enzyme and 6-phosphogluconate dehydrogenase were decreased by 79% and 67% respectively (Figure 14). ATP citrate lyase, immediately upstream of ACC1, was decreased by 61% (Figure 13).

Genes that were partially or fully restored in the refed *L-ChREBP*$^{-/-}$ mice injected with AAV-SREBP-1c relative to refed *L-ChREBP*$^{-/-}$ mice injected with AAV-GFP include glycerol-3-phosphate acyltransferase, which, compared to fasted controls, overshot 12-fold in refed control mice but only 7-fold in *L-ChREBP*$^{-/-}$ mice receiving AAV-SREBP-1c, a 44% reduction. Likewise, SCD-1 overshot 4-fold in the refed control mice and 3-fold in the AAV-SREBP-1c *L-ChREBP*$^{-/-}$ mice, a 28% reduction.

ACC2 was nearly fully restored (Figure 14). ACSS2 (Figure 14) and G6PD (Figure 15) overshot the refed control levels by 27% and 145% respectively. Therefore, ACC2, ACSS2 and G6PD are dependent on SREBP-1c for activation, and their lack of induction upon refeeding in *L-ChREBP*$^{-/-}$ mice is due to the secondary decrease in nuclear SREBP-1, not due to the ChREBP knockout.

mRNA induction of NADPH-producing genes in AAV-injected mice

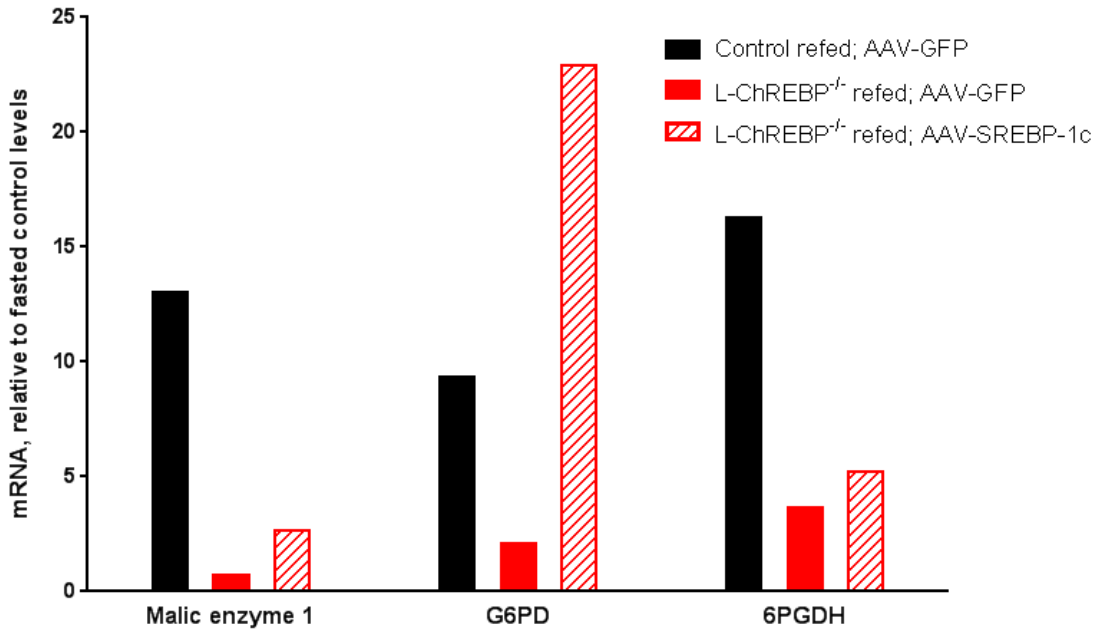

Figure 14: mRNA induction of NADPH-producing enzymes in AAV-GFP control mice, AAV-GFP *L-ChREBP*$^{-/-}$ mice, and AAV-SREBP-1c *L-ChREBP*$^{-/-}$ mice

The genes responsible for NADPH synthesis show different responses to the administration of AAV-SREBP-1c. All three genes were dramatically decreased in *L-ChREBP*$^{-/-}$ mice, but show two different responses to SREBP-1c injection. Glucose-6-phosphate dehydrogenase was strongly stimulated by SREBP-1c injection, while both malic enzyme and 6-phosphogluconate showed little transcriptional response to increased nuclear SREBP-1c.

mRNA induction of cholesterol-producing genes in AAV-injected mice

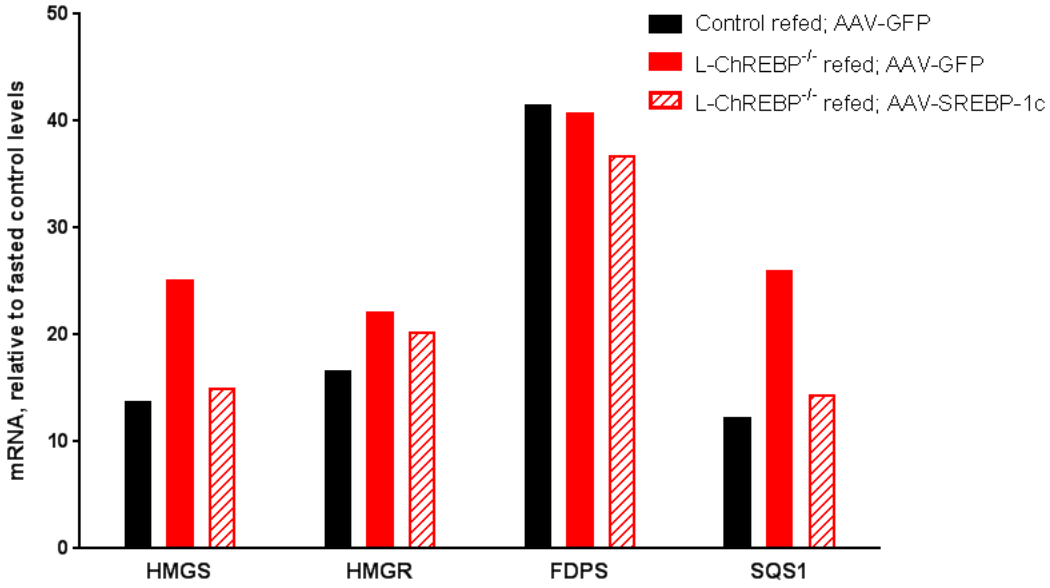

Figure 15: mRNA induction of cholesterol-producing enzymes in AAV-GFP control mice, AAV-GFP *L-ChREBP*$^{-/-}$ mice, and AAV-SREBP-1c *L-ChREBP*$^{-/-}$ mice

Regarding genes of the sterol biosynthetic pathway, the injection of AAV-SREBP-1c did not have large effects on HMG-CoA reductase and farnesyl diphosphate synthase mRNA levels, but did decrease HMG-CoA synthase and squalene synthase slightly (Figure 15). In no cholesterol-synthesizing genes did AAV-SREBP-1c increase the refed mRNA level, consistent with previous studies demonstrating that SREBP-2, rather than SREBP-1c, controls sterologenic transcription (Liang et al., 2002).

Table 4

Effects of fasting and refeeding on AAV-injected control and *L-ChREBP*$^{-/-}$ mice

	Control		***L-ChREBP*$^{-/-}$**		
Parameter	**Fasted**	**Refed**	**Fasted**	**Refed**	**Refed**
AAV type	GFP	GFP	GFP	GFP	SREBP-1c
Number of mice	5	6	4	4	5
Body weight (g)	24.7 ± 1.0	22.1 ± 0.4	23.6 ± 0.8	21.2 ± 0.5	20.2 ± 0.8
Liver weight (g)	1.1 ± 0.05	1.4 ± 0.04	1.0 ± 0.02	1.4 ± 0.07	1.5 ± 0.09
Liver weight/body weight (%)	4.3 ± 0.12	6.4 ± 0.19	4.4 ± 0.18	6.6 ± 0.20	7.6 ± 0.16**
Liver cholesterol content (mg/g)	2.42 ± 0.05	1.60 ± 0.08	3.01 ± 0.36	1.35 ± 0.06	2.00 ± 0.13*
Liver triglyceride content (mg/g)	86 ± 8.6	6.3 ± 0.7	117.4 ± 14.5	8.5 ± 1.5	37.0 ± 3.9**
Liver glycogen content (mg/g)	2.0 ± 0.4	68.2 ± 7.3	4.3 ± 1.7	78.2 ± 7.3	82.3 ± 7.4
Total plasma cholesterol (mg/dL)	129 ± 1	79 ± 2	96 ± 6**	60 ± 2**	59 ± 7*
Total plasma triglyceride (mg/dL)	118 ± 6	118 ± 8	109 ± 2	79 ± 9*	76 ± 10*
Plasma non-esterified fatty acids (mM)	1.23 ± 0.08	0.31 ± 0.03	1.12 ± 0.10	0.31 ± 0.05	0.58 ± 0.10*
Plasma aspartate transaminase (U/L)	146 ± 17	115 ± 13	117 ± 12	132 ± 28	197 ± 23**
Plasma alanine transaminase (U/L)	38 ± 2	40 ± 3	47 ± 3*	62 ± 3**	113 ± 32*
Plasma insulin (ng/mL)	0.52 ± 0.05	2.36 ± 0.62	0.55 ± 0.04	1.31 ± 0.14	0.85 ± 0.07
Plasma glucose (mg/dL)	63 ± 3	123 ± 7	77 ± 7	121 ± 4	117 ± 8

Control and *L-ChREBP*$^{-/-}$ littermates (male, 8 weeks of age) were injected via the tail vein with recombinant AAV-GFP or AAV-nSREBP1c ($2x10^{11}$ gene copies per mouse). Seven days after the injection, the mice were subjected to fasting (F) and refeeding (R). The fasted group was fasted 12 h, and the refed group was fasted for 12 h and then refed a high sucrose/fat-free diet for 12 h prior to study. The starting times for the feeding regimens were staggered so that all mice were sacrificed at the same time, which was at the end of the dark cycle. Each value represents the mean ± SEM. Asterisks denote the level of statistical significance between control and *L-ChREBP*$^{-/-}$ of the same dietary treatment. *P<0.05 and **P<0.01.

Blood plasma metabolites

Plasma cholesterol was decreased in the refed state relative to the fasted state in both genotypes. Fasted *L-ChREBP*$^{-/-}$ mice had lower plasma cholesterol levels than control mice, and refed *L-ChREBP*$^{-/-}$ mice had lower plasma cholesterol levels than refed control mice. Plasma triglycerides were unchanged in control mice regardless of feeding conditions. In *L-ChREBP*$^{-/-}$ refed mice, plasma triglycerides were decreased compared to refed control mice. Plasma free fatty acids were elevated in the fasted condition compared to all refed conditions. No significant differences were found between the two *L-ChREBP*$^{-/-}$ refed groups, but refed

AAV-SREBP-1c *L-ChREBP*$^{-/-}$ mice had free fatty acids 84% higher than refed AAV-GFP control mice. Aspartate aminotransferase levels were elevated 72% in refed *L-ChREBP*$^{-/-}$ AAV-SREBP-1c mice compared to refed control AAV-GFP mice, but no other differences among groups were observed.

Alanine aminotransferase levels in blood plasma were normal in all AAV-GFP injected mice. Refed *L-ChREBP*$^{-/-}$ mice had higher ALT levels than refed control mice. The difference between refed AAV-GFP *L-ChREBP*$^{-/-}$ mice and refed AAV-SREBP-1c *L-ChREBP*$^{-/-}$ mice was not significant, suggesting that AAV-SREBP-1c does not induce excess liver inflammation compared to AAV-GFP.

Liver triglycerides, cholesterol, and glycogen

Liver triglycerides and cholesterol were increased in the fasted conditions and decreased in the refed conditions. Additionally, the refed *L-ChREBP*$^{-/-}$ AAV-SREBP-1c mice had increased liver cholesterol and triglycerides compared to control AAV-GFP and *L-ChREBP*$^{-/-}$ AAV-GFP refed mice. Liver glycogen was elevated in the refed condition compared to the fasted condition, but no statistically significant differences were found among mice subjected to the same feeding condition.

CHAPTER THREE
Discussion

INTERPRETATION OF EXPERIMENTAL RESULTS

The liver-specific ChREBP knockout mice showed large decreases in the mRNA levels of all lipogenic genes. However, they appeared grossly normal, and the levels of various plasma metabolites in *L-ChREBP*$^{-/-}$ mice were generally similar to those found in control mice. This suggests that the ChREBP present in other tissues, particularly the white adipose tissue, allows the mice to compensate for the loss of hepatic ChREBP to maintain normal health and biological functions. Additionally, alanine aminotransferase and aspartate aminotransferase levels were in the healthy range, indicating that the deletion of ChREBP in the liver does not cause major liver injury.

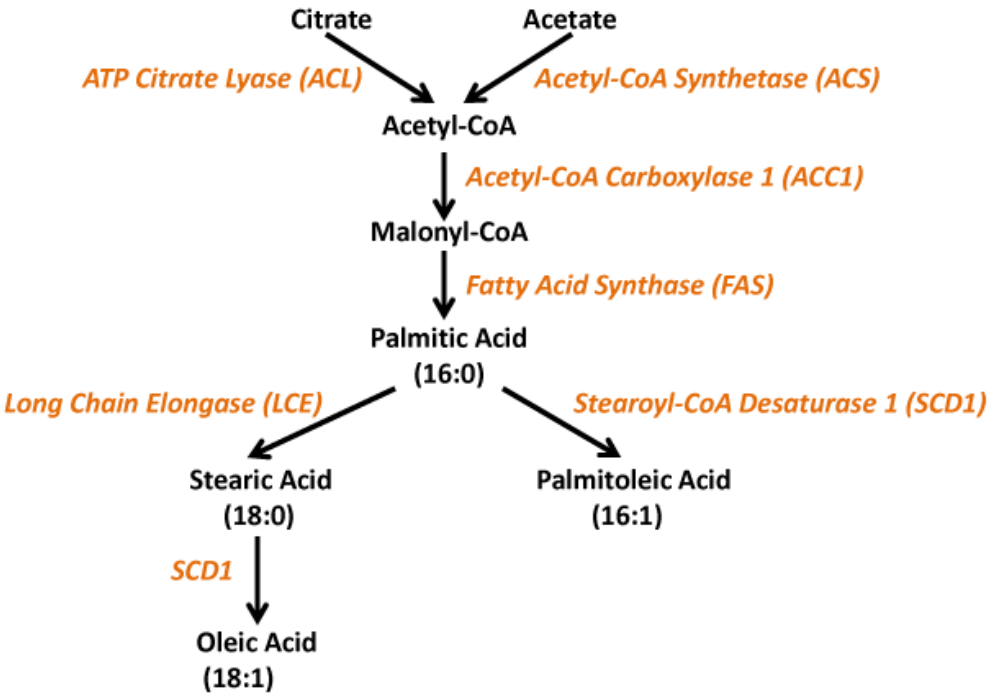

Figure 16: The lipogenic pathway

Using an adeno-associated virus to restore nuclear SREBP-1 levels, I was able to categorize lipogenic genes into three types: 1. genes not restored by SREBP-1c in the absence of ChREBP; 2. genes partially restored by SREBP-1c in absence of ChREBP; 3. genes fully restored by SREBP-1c in the absence of ChREBP. Genes of the third type are predominantly dependent upon SREBP-1c for their transcription since normalization of SREBP-1c in the absence of ChREBP restores their transcription. Since the single loss of either ChREBP or SREBP-1c reduces levels of type 1 and 2 genes, and since they are not fully restored by normalizing SREBP-1c in the *L-ChREBP*$^{-/-}$ mice, they require both ChREBP and SREBP-1c for full post-prandial transcriptional induction.

Genes not restored by AAV-SREBP-1c were ACC1, FASN, and ELOVL6. These genes are centrally located in the lipogenic pathway (Figure 16). Other lipogenic genes that were not restored by the injection of AAV-SREBP-1c include ACLY, ME1, and 6PGDH. ACLY generates Acetyl-CoA, and ME1 and 6PGDH generate NADPH. These genes, as a group, require both an intact ChREBP and SREBP-1 for normal postprandial stimulation.

On the other hand, several lipogenic genes were completely restored by the AAV-SREBP-1c, suggesting that their transcription is primarily dependent on SREBP-1c rather than ChREBP. ACSS2, ACC2, SCD1, and G6PD all showed complete or nearly complete restoration of refeeding induction in *L-ChREBP*$^{-/-}$, AAV-SREBP-1c-injected mice compared to control, AAV-GFP-injected mice.

Acetyl-CoA synthetase generates acetyl-CoA from acetate, serving to produce acetyl-CoA from a different source than ATP citrate lyase. Acetyl-CoA carboxylase 2, also known as acetyl-CoA carboxylase beta, produces malonyl-CoA in the mitochondria, which inhibits

the carnitine palmitoyltransferase I shuttle required to import fatty acids into the mitochondria for oxidation. Thus, rather than playing a direct role in fatty acid synthesis, the induction of ACC2 during lipogenesis prevents the cell from catabolizing the newly generated energy stores, which would lead to the waste of metabolic energy.

Stearoyl-CoA desaturase is responsible for converting stearate into oleate, and glucose-6-phosphate dehydrogenase generates NADPH in the rate-limiting step of the pentose phosphate pathway. Unlike the other two NADPH-producing genes (ME1 and 6PGDH), G6PD is dependent on SREBP-1c. That SREBP-1c and ChREBP activate different genes responsible for lipogenesis and the production of necessary cofactors confirms that both ChREBP and SREBP-1c are necessary to induce lipogenesis.

Slight increases in mRNA levels of LXR alpha, LXR beta, ABCG5 and ABCG8 were observed in *L-ChREBP*$^{-/-}$ mice compared to control mice under similar feeding conditions (Table 3), suggesting that the decrease in lipogenic gene transcription was not due to a decrease in LXR. Levels of SREBP-2-regulated genes were also mildly elevated in *L-ChREBP*$^{-/-}$ mice, possibly as a result of less competition for precursor SREBP-2 with precursor SREBP-1 for Scap binding in the ER.

To more fully elucidate the lipogenic picture, our laboratory is currently carrying out experiments to confirm that the truncated ChREBP protein produced in *L-ChREBP-/-* mice is biologically inert. The truncation lacks the dimerization and DNA-binding domains, so we do not expect it to be capable of affecting mRNA regulation or binding to Mlx, the normal binding partner of ChREBP.

The regulation of the transcription of lipogenic genes is a complex process, affected by signaling pathways that assay the levels of various sources of energy (free carbohydrates, liver and muscle glycogen, stored fatty acids in adipose tissue, excess protein that can be catabolized, etc.) that an organism can access. The conversion of carbohydrate to fatty acids involves the expenditure of metabolic energy during the processes of lipogenesis, triglyceride transport, storage in adipose tissue, and catabolism. Therefore, while the storage of excess carbohydrates of fatty acids is an essential tool for the survival of complex organisms, its careful regulation to prevent unnecessary energetic loss is essential. LXR, ChREBP and SREBP-1c are involved in an intricate, cooperative balance in lipogenic regulation.

CHAPTER FOUR
Experimental Procedures

METHODOLOGY

Mouse Lines

C57/Black6 mice were obtained from The Jackson Laboratory (Bar Harbor, Maine). *L-ChREBP*$^{-/-}$ mice were generated by Guosheng Liang of the UT Southwestern Department of Molecular Genetics. *ChREBP*$^{-/-}$ mice were previously described (Iizuka et al., 2004).

Generation of liver-specific *ChREBP* knockout mice (*L-ChREBP*$^{-/-}$)

A conditional targeting vector of a replacement type was produced by the insertion of a *loxP* site 150 bp upstream of exon 9 and a *loxP*, *frt*-flanked *pgkneopA* cassette immediately downstream of exon 15. LR-2 ES cells, derived from albino C57BL6/J blastocysts, were cultured on leukemia inhibitory factor-producing STO feeder cells and transfected with the linearized targeting vector as described previously (Engelking et al., 2004). Three positive ES clones were expanded and injected into C57BL/6J blastocysts to obtain chimeric males. All resulting chimeric males were used to cross to C57BL/6NCrl females to obtain offspring that carries the floxed *ChREBP* conditional allele with the *loxP*, *frt*-flanked *pgkneopA* cassette (*ChREBP*$^{+/fneo}$) through the germ line. Since the presence of the *pgkneopA* cassette causes constitutive germline deletion of ChREBP (data not shown), we bred the *ChREBP*$^{+/fneo}$ mice with a strain of transgenic mice that express a *FLP1* recombinase gene under the direction of the human *ACTB* promoter (Jackson Laboratory, No. 003800) to remove the *frt*-flanked *pgkneopA* cassette. The resulting *ChREBP*$^{+/f}$ mice were then

intercrossed to produce mice homozygous for the floxed allele without the selection cassette (*ChREBP*$^{f/f}$). *ChREBP*$^{f/f}$ mice were bred to *Albumin-Cre* transgenic mice in the C57/Black6 background (Jackson Laboratory, No. 003574) that express Cre recombinase driven from the albumin promoter (*Alb*-Cre) to generate mice homozygous for the floxed *ChREBP* allele and hemizygous for the *Alb*-Cre transgene (*ChREBP*$^{f/f}$*;Alb-Cre*). For brevity, we designated the *ChREBP*$^{f/f}$*;Alb-Cre* mice as *L-ChREBP*$^{-/-}$ (liver-specific *ChREBP* knockout). Littermate *ChREBP*$^{f/f}$ mice were used as controls for all of the experiments.

General care and housing of mice

All animal experiments were performed with the approval of the Institutional Animal Care and Use Committee of the University of Texas Southwestern Medical Center. Under standard conditions, mice were housed with a 12 hour/12 hour day/night cycle, with 9AM – 9 PM in light and 9 PM – 9 AM in darkness. With the exception of mice under immediate experimental alteration of diet and feeding patterns, mice were provided ad libitum access to Harlan Laboratories Teklad 2018 Global 18% Protein Rodent Diet (Harlan Labs catalog # 2018) as well as water. Cages were changed a minimum of once weekly.

Generation and tail vein injection of adeno-associated virus

The nucleic acid sequence encoding a Kozak sequence, start codon, and amino acids 1-456 of mouse SREBP-1c followed by a stop codon was cloned into the multiple cloning site of an AAV plasmid containing a CAG promoter. Expression with AAV helper plasmids in QBI-293A cells yielded AAV-SREBP-1c. The CAG promoter is a hybrid of the

cytomegalovirus and chicken beta-actin promoters. After initial testing to confirm increased nuclear SREBP-1c expression in AAV-SREBP-1c injected *L-ChREBP*$^{-/-}$ mice, this AAV plasmid was provided to Vector Biolabs (Malvern, PA) for large-scale synthesis using the AAV-DJ packaging, which is liver-specific. A similar AAV-DJ expressing enhanced GFP under the CAG promoter was used as a control virus (AAV-GFP).

Purified AAV-DJ of the appropriate type was diluted using phosphate buffered saline to a concentration such that a 200 uL injection would contain one dose ($2x10^{11}$ gene copies). A mouse was moved to a clean cage under a heat lamp for 3 minutes and then was placed in a restraining device. The mouse's tail was washed with ethanol to disinfect the injection site and the tail vein was visually identified on the lateral aspect of the tail. The tail was bent 20 degrees at the injection site to accommodate the needle tip. 200 uL of virus/PBS solution was injected and needle placement in the vein was confirmed by visual observation of blanching in the vein. Following injection, the needle was removed and the injection site was placed under light pressure with gauze for 20-30 seconds to allow clotting of the wound. The mouse was then moved to a fresh cage with food and water available. Needle dead volume was accounted for by leaving a small excess of virus solution in the needle. Becton Dickinson 1 mL syringes (BD catalog # 309659) and Becton Dickinson PrecisionGlide 25G needle tips (BD catalog # 305109) were used.

Mice injected with AAV were sacrificed eight days later at 9 AM at the beginning of the light cycle, after the appropriate alterations in feeding regimen.

Alteration of mouse metabolism for experimental observation: 12-hour fasting and refeeding

In experiments denoted as taking place following a 12-hour fast or a 12-hour fast and 12-hour refeeding, mice were subjected to certain restrictions on food intake:

Nonfasted: Mice were allowed ad lib access to standard Global 18% Protein Rodent Diet until sacrifice at 9 AM.

Fasted: Mice were fasted beginning at 9 PM on the evening prior to sacrifice. They were sacrificed at 9 AM the following morning, and blood glucose, plasma metabolites, and liver mRNAs and protein levels were measured.

Refed: Mice were fasted at 9 AM, 24 hours prior to sacrifice. They were refed at 9 PM with a large (>15 grams) amount of Fat-Free Diet, Modified (MP Biomedicals catalog # 02960238). Mice were sacrificed at 9 AM the following morning, after a 12 hour period of food availability. The amount of food consumed in the 12 hour period by each mouse in a refed group was measured.

Procedure for mouse sacrifice and tissue/blood sample collection

Mice were transported in covered cages from the UT Southwestern Animal Resource Center to the animal procedure room of the UT Southwestern Department of Molecular Genetics (L5.254). Blood glucose was measured by nicking the tail with a razor blade and measuring a drop of blood with a Bayer Contour Blood Glucose Measuring System (Bayer catalog # 82486543). Mice were anesthetized using isofluorane (Henry Schein Animal Health catalog # 050033). Following anesthetization, an incision into the peritoneum was

made and 400 µL blood removed from the inferior vena cava using a Becton Dickinson 1 mL syringe (BD catalog # 309659) and Becton Dickinson PrecisionGlide 23G1 needle (BD catalog # 305145). Blood was placed in EDTA-coated tubes (Sarstedt product no. 20.1341.100) on ice to await collection of all samples, then spun at 8000 rpm in a cooled Eppendorf 5424R centrifuge (Eppendorf product #5404000.413) for 10 minutes at 4 degrees to isolate plasma. Fresh plasma was submitted to the UTSW Metabolic Core for analysis, and the remaining plasma was frozen at -80 degrees for future use. The liver was separated using surgical scissors from surrounding tissues and immediately frozen in liquid nitrogen (Airgas, Inc.)

Blood metabolite assays

Plasma cholesterol, triglycerides, non-esterified fatty acids, AST, and ALT assays were done by the UT Southwestern Metabolic Core (Y5.222). Plasma insulin concentrations were measured using an Ultra Sensitive Mouse Insulin ELISA Kit (Crystal Chem Inc. catalog # 90080).

Liver glycogen assay

Liver glycogen levels were measured using a BioVision Glycogen Colorimetric/Fluorometric Assay Kit (BioVision catalog # K646-100). 100 mg of liver tissue was homogenized in water at full speed for 10 seconds with a Pro Scientific Inc. BioGen PRO200 Homogenizer (Pro Scientific catalog # 01-01200), then kept on ice. The resulting

lysate was diluted tenfold with water and then subjected to BCA assay for protein quantification and the glycogen assay per kit instructions.

Liver cholesterol and liver triglycerides assay

Liver triglycerides and cholesterol concentrations were measured as previously described (Engelking et al., 2004).

Isolation and preparation of protein for immunoblotting

100 mg of frozen liver tissue was placed in 1.5 mL ice-cold whole cell lysate buffer in a Bectin Dickinson 14 mL Polypropylene Round-Bottom Tube (BD catalog # 352059). Whole cell lysate (WCL) buffer consists of 1% w/v sodium dodecyl sulfate, 1% w/v Triton X-100, 1% w/v NP-40, 50 mM Tris-HCl (pH 7.4), 5 mM EDTA in deionized water. Tissue and WCL buffer was homogenized at full speed for 10 seconds with a Pro Scientific Inc. BioGen PRO200 Homogenizer (Pro Scientific catalog # 01-01200), then returned to ice. The resulting lysate was spun down at 3700 rpm in a Thermo Scientific Sorvall RT+ centrifuge (Thermo Scientific catalog # 750004377) for 10 minutes to remove insoluble debris. Supernatant was isolated and the protein concentration measured via BCA assay. Supernatant was then added in a 3:1 ratio to 4x Laemmli sample buffer (12% SDS, 0.02% bromophenol blue, 30% glycerol, 0.15 M Tris-Cl, pH 6.8) and boiled at 95 degrees for 5 minutes. After protein concentration was determined, the protein/Laemmli buffer mixture was diluted with 1x Laemmli buffer to 2 mg/mL, and a volume of 15 uL (containing 30 µg protein) was run in each lane of an SDS-PAGE gel for analysis.

Primary antibodies

Anti-ChREBP antibody was obtained from Novus Biologicals (Novus catalog no. NB400-135). Polyclonal anti-SREBP-1, anti-SREBP-2, anti-Insig-1, anti-Insig-2, and anti-SCAP antibodies were generated by the UT Southwestern Molecular Genetics department. Anti-GFP antibody was purchased from Novus (Novus catalog no. NB600-303). Anti-calnexin antibody was purchased from Novus (Novus catalog no. NB100-1974).

All primary antibodies except calnexin were diluted 1:2000 in a solution of 5% BSA, 1% FCS, and 0.002% sodium azide in phosphate-buffered saline containing 0.05% Tween-20 at pH 7.4. Calnexin was diluted 1:30000, and all other concentrations of solutes were equal to other antibodies.

Secondary antibodies

ECL Anti-Rabbit IgG, Horseradish peroxidase linked whole antibody was obtained from GE Healthcare Life Sciences (GE Healthcare catalog # NA934V). The antibody was diluted 2:5000 into a 5% dried milk w/v (Member's Mark Nonfat Dry Milk), 5% fetal calf serum v/v mixture in phosphate-buffered saline with 0.05% Tween-20, pH 7.4 (Sigma Aldrich catalog # P3563-10PAK).

SDS-PAGE gels

Standard 8%, 10% and 12% SDS-PAGE gels were run in a Bio-Rad Mini Protean Tetra Cell (Bio-Rad catalog # 165-8004EDU) with buffer diluted from Bio-Rad 10x

Tris/Glycine/SDS buffer (Bio-Rad catalog # 161-0772). The molecular size marker used was Precision Plus Protein™ Kaleidoscope™ (Bio-Rad catalog # 161-0375).

For blots that required particularly fine molecular weight resolution, NuPAGE 4-12% Bis-Tris Gels (Novex catalog # NP0321BOX) were used, purchased from Novex by Life Technologies. These gels were run with Novex MES SDS Running Buffer (Novex catalog # NP0002) in a Life Technologies X-Cell SureLock™ Mini-Cell Electrophoresis System (Life Technologies catalog # EI0001).

Radiogram exposures

After electrophoresis, SDS-PAGE gels were transferred to nitrocellulose membranes (BioRad product # BR20140312) using Trans-Blot Turbo Midi-size Transfer Stacks (BioRad product # BR20140316) in a Bio-Rad TransBlot Turbo Transfer Starter System (Bio-Rad product # 170-4155). The transfer was done for 15 minutes at 2.5 amps. Membranes were then stained with Ponceau S solution (Sigma Aldrich catalog # P7170-1L) for 3 minutes. A visual inspection of the membrane was made to ensure no bubbles or areas of defective protein transfer were observed. High quality membranes were then transferred to the blocking step.

Blocking: Membranes were blocked for 2 hours, in a 5% dried milk w/v (Member's Mark Nonfat Dry Milk), 5% fetal calf serum v/v mixture in phosphate-buffered saline with 0.05% Tween-20, pH 7.4 (Sigma Aldrich catalog # P3563-10PAK). 200 mL of milk/FCS/PBST mixture was placed in a closed container into which the membranes were placed, then shaken at a moderate pace (40 rpm).

Washing: The container was emptied of milk/FCS/PBST mixture and pure PBST was added to the container. The membranes were shaken for 1 hour and the PBST was changed every 20 minutes.

Primary: Primary antibody stock solutions (described above) were pipetted into small lidded dishes measuring 6 cm by 6 cm. Membranes were transferred into these dishes and shaken overnight (slowly, 20 rpm)

Washing: Primary antibody was removed from the lidded dishes and returned to storage at 4 degrees. PBST was added to the dishes, and they were shaken vigorously (60 rpm) for 1 hour. During this time PBST was changed every 10 minutes.

Secondary: PBST was removed from the dishes and secondary antibodies (described above) were added to the dishes for 1 hour.

Washing: Secondary antibody was removed from the dishes and discarded. PBST was added to the dishes and they were shaken vigorously (60 rpm) for 1 hour. PBST was changed every 15 minutes during this time.

Luminol: PBST was removed from the dishes and 15 mL of SuperSignal West Pick Chemiluminescent Substrate (Thermo Scientific catalog # 34080) was added to the dishes. Dishes were shaken at intermediate speed (30 rpm) for 5 minutes.

Radiogram exposure and quantification: Fluorescence was recorded using a Li-COR Odyssey Fc imaging system. Exposures of membranes were done for 2 minutes on the chemiluminescence setting to detect protein bands and 2 minutes at 700 nm to image the ladder.

ACKNOWLEDGEMENTS

I would like to thank my mentors, Michael Brown and Joseph Goldstein, for their insightful suggestions and scientific guidance. It was a privilege to work in their laboratory, and their unmatched expertise in the fields of cholesterol and lipid metabolism was completely essential to this work. I have no doubt that the standard of scientific rigor that I have learned from them will serve me well in my future research endeavors.

My dissertation committee, Joyce Repa, Jay Horton, and Jin Ye, were an extraordinary resource. All three have extensive experience with the transcription factors that I studied, and their helpful comments and critiques of my experiments and research direction were invaluable.

I would like to thank Guosheng Liang for his constant advice and encouragement. Dr. Liang is our laboratory's resident expert on mouse breeding, animal surgery, and the experimental quantification of metabolites. All experiments performed in this paper benefited immensely from his oversight and guidance, and would not have been possible without his assistance.

Luke Engelking, a former MSTP from the Brown/Goldstein lab who has since returned to UT Southwestern to begin his own research group, also provided helpful and incisive comments on many of my experiments.

I would also like to thank the following members of the Department of Molecular Genetics who assisted with my research: Hwa Choi, Isis Soto, Min Ding, Linda Donnelly, Angela Carroll, and Jeffry Cormier.

APPENDIX A
qPCR primers for mRNA quantification

Gene	Sequence of forward and reverse primers (5'-3')
ApoB	CGTGGGCTCCAGCATTCTA TCACCAGTCATTTCTGCCTTTG
ChREBP, knockout deleted region	GCCTCCGCCAGACCTCACTG AGTGCTGAGTTGGCGAAGGG
ChREBP-α	CGACACTCACCCACCTCTTC TTGTTGAGCCGGATCTTGTC
ChREBP-β	TCTGCAGATCGCGTGGAG CTTGTCCCGGCATAGCAAC
L-type pyruvate kinase	GGCATCGAAAGTGGAAAGCT GCCAGCCTGTCACCACAAT
Glut-2	TTGACTGGAGCCCTCTTGATG CACTTCGTCCAGCAATGATGA
Glucokinase	CCGTGATCCGGGAAGAGAA GGGAAACCTGACAGGGATGAG
Fructokinase (Ketohexokinase)	CGTGAGGAGCTCTTCCAGTTG CAGGTGCTTGGCCACATCT
Triose kinase	GCCGGGTAGCACTTCTGTCA TTAGCATCCCTTTCCCGATAAA
PEPCK	CCACAGCTGCTGCAGAACA GAAGGGTCGCATGGCAAA
Glucose-6-phosphatase	TGGGCAAAATGGCAAGGA TCTGCCCCAGGAATCAAAAAT
Scap	ATTTGCTCACCGTGGAGATGTT GAAGTCATCCAGGCCACTACTAATG

SREBP-1a	GGCCGAGATGTGCGAACT TTGTTGATGAGCTGGAGCATGT
SREBP-1c	GGAGCCATGGATTGCACATT GGCCCGGGAAGTCACTGT
SREBP-2	GCGTTCTGGAGACCATGGA ACAAAGTTGCTCTGAAAACAAATCA
Insig-1	TCACAGTGACTGAGCTTCAGCA TCATCTTCATCACACCCAGGAC
Insig-2a	CCCTCAATGAATGTACTGAAGGATT TGTGAAGTGAAGCAGACCAATGT
Insig-2b	CCGGGCAGAGCTCAGGAT GAAGCAGACCAATGTTTCAATGG
ATP citrate lyase	GCCAGCGGGAGCACATC CTTTGCAGGTGCCACTTCATC
Acetyl-CoA synthetase	GCTGCCGACGGGATCAG TCCAGACACATTGAGCATGTCAT
Acetyl-CoA carboxylase 1	TGGACAGACTGATCGCAGAGAAAG TGGAGAGCCCCACACACA
Acetyl-CoA carboxylase 2	GGGCTCCCTGGATGACAAC GCTCTTCCGGGAGGAGTTCT
Fatty acid synthase	GCTGCGGAAACTTCAGGAAAT AGAGACGTGTCACTCCTGGACTT
Long chain fatty acyl elongase 6	TGTACGCTGCCTTTATCTTTGG GCGGCTTCCGAAGTTCAA
Stearoyl-CoA desaturase-1	CCGGAGACCCCTTAGATCGA TAGCCTGTAAAAGATTTCTGCAAACC
Glycerol-3-phosphate acyltransferase	CAACACCATCCCCGACATC GTGACCTTCGATTATGCGATCA
Malic enzyme	GCCGGCTCTATCCTCCTTTG

	TTTGTATGCATCTTGCACAATCTTT
Glucose-6-phosphate dehydrogenase	GAACGCAAAGCTGAAGTGAGACT TCATTACGCTTGCACTGTTGGT
6-phosphogluconate dehydrogenase	AGGCCCTCTATGCTTCCAAGA CTCAGTGGCTGCCTGTCTGA
HMG-CoA synthase	GCCGTGAACTGGGTCGAA GCATATATAGCAATGTCTCCTGCAA
HMG-CoA reductase	CTTGTGGAATGCCTTGTGATTG AGCCGAAGCAGCACATGAT
FDP synthase	ATGGAGATGGGCGAGTTCTTC CCGACCTTTCCCGTCACA
Squalene synthase	CCAACTCAATGGGTCTGTTCCT TGGCTTAGCAAAGTCTTCCAACT
LDL receptor	AGGCTGTGGGCTCCATAGG TGCGGTCCAGGGTCATCT
PCSK9	CAGGCGGCCAGTGTCTATG GCTCCTTGATTTTGCATTCCA
LXRα	TCTGGAGACGTCACGGAGGTA CCCGGTTGTAACTGAAGTCCTT
LXRβ	CTCCCACCCACGCTTACAC GCCCTAACCTCTCTCCACTCA
ABCA1	CGTTTCCGGGAAGTGTCCTA GCTAGAGATGACAAGGAGGATGGA
ABCG5	TGGATCCAACACCTCTATGCTAAA GGCAGGTTTTCTCGATGAACTG
ABCG8	TGCCCACCTTCCACATGTC ATGAAGCCGGCAGTAAGGTAGA

REFERENCES

Apfel R., Benbrook D., Lernhardt E., Ortiz M.A., Salbert G., Pfahl M. (1994). A Novel Orphan Receptor Specific for a Subset of Thyroid Hormone-Responsive Elements and Its Interaction with the Retinoid/Thyroid Hormon Receptor Subfamily. Mol Cell Bio *14*, 7025-7035.

Brown M.S. and Goldstein J.L. (1999). A proteolytic pathway that controls the cholesterol content of membranes, cells, and blood. Proc Natl Acad Sci U S A *96*, 11041-11048.

Brown M.S. and Goldstein J.L. (1997). The SREBP Pathway: Regulation of a Cholesterol Metabolism by Proteolysis of a Membrane-Bound Transcription Factor. Cell *89*, 331-340.

Burgess S.C., Iizuka K., Jeoung N.H., Harris R.A., Kashiwaya Y., Veech R.L., Kitazume T., Uyeda K. (2008). Carbohydrate-response Element-binding Protein Deletion Aletrs Substrate Utiliazation Producing an Energy-deficient Liver. J Biol Chem *283*, 1670-1678.

Cha J. and Repa J.J. (2007). The Liver X Receptor (LXR) and Hepatic Lipogenesis. J Biol Chem *282*, 743-751.

Chu K., Miyazaki M., Man W.C., Ntambi J.M. (2006). Stearoyl-Coenzyme A Desaturase 1 Deficiency Protects against Hypertriglyceridemia and Increases Plasma High-Density Lipoprotein Cholesterol Induced by Liver X Receptor Activation. Mol Cell Bio *26*, 6786-6798.

DeBose-Boyd R.A., Ou J., Goldstein J.L., Brown M.S. (2001) Expression of sterol regulatory element-binding protein 1c (SREBP-1c) mRNA in rat hepatoma cells requires endogenous LXR ligands. Proc Natl Acad Sci U S A *98*, 1477-1482.

DeBose-Boyd R.A., Brown M.S., Li W., Nohturfft A., Goldstein J.L., Espenshade P.J. (1999). Transport-Dependent Proteolysis of SREBP: Relocation of Site-1 Protease from Golgi to ER Obviates the Need for SREBP Transport to Golgi. Cell *99*, 703-712.

Engelking L.J., Kuriyama H., Hammer R.E., Horton J.D., Brown M.S., Goldstein J.L., Liang G. (2004). Overexpression of Insig-1 in the livers of transgenic mice inhibits SREBP processing and reduces insulin-stimulated lipogenesis. J Clin Invest *113*, 1168-1175.

Forman B.M., Ruan B., Chen J., Schroepfer G.J., Evans R.M. (1997). The orphan receptor LXRα is positively and negatively regulated by distinct products of mevalonate metabolism. Proc Natl Acad Sci U S A *94*, 10588-10593.

Fukasawa M., Ge Q., Wynn R.M., Ishii S., Uyeda K. (2010). Coordinate regulation/localization of the carbohydrate responsive binding protein (ChREBP) by two nuclear export signal sites: Discovery of a new leucine-rish neculear export signal site. Biochem. and Biophys. Res. Comm. *391*, 1166-1169.

Goldstein J.L. and Brown M.S. (1990). Regulation of the mevalonate pathway. Nature *343*, 425-430.

Herman M.A., Peroni O.D., Villoria J., Schön M.R., Abumrad N.A., Blüher M., Klein S., Kahn B.B. (2012). A novel ChREBP isoform in adipose tissue regulates systemic glucose metabolism. Nature *484*, 333-338.

Horton J.D., Goldstein J.L., Brown M.S. (2002). SREBPs: activators of the complete program of cholesterol and fatty acid synthesis in the liver. J Clin Invest *109*, 1125-1131.

Hua X., Sakai J., Brown M.S., Goldstein J.L. (1996). Regulated Cleavage of Sterol Regulatory Element Binding Proteins Requires Sequences on Both Sides of the Endoplasmic Reticulum Membrane. J Biol Chem *271*, 10379-10384.

Hua X., Wu J., Goldstein J.L., Brown M.S., Hobbs H.H. (1995). Structure of the Human Gene Encoding Sterol Regulatory Element Binding Protein-1 (*SREBF1*) and Localization of *SREBF1* and *SREBF2* to Chromosomes 17p11.2 and 22q13. Genomics *26*, 667-673.

Hua X., Yokoyama C., Wu J., Briggs M.R., Brown M.S., Goldstein J.L., Wang X. (1993). SREBP-2, a second basic-helix-loop-helix-leucine zipper protein that stimulates transcription by binding to a sterol regulatory element. Proc Natl Acad Sci U S A *90*, 11603-11607.

Iizuka K., Bruick R.K., Liang G., Horton J.D., Uyeda K. (2004). Deficiency of carbohydrate response element-binding protein (ChREBP) reduces lipogenesis as well as glycolysis. Proc Natl Acad Sci U S A *101*, 7281-7286.

Iizuka K., Miller B., Uyeda K. (2006). Deficiency of carbohydrate-activated transcription factor ChREBP prevents obesity and improves plasma glucose control in leptin-deficient (*ob/ob*) mice. Am J Physiol Endocrinol Metab *291*, E358-E364.

Ishii S., Iizuka K., Miller B.C., Uyeda K. (2004). Carbohydrate response element binding protein directly promotes lipogenic enzyme gene transcription. Proc Natl Acad Sci U S A *101*, 15597-15602.

Janowski B.A., Grogan M.J., Jones S.A., Wisely G.B., Kliewer S.A., Corey E.J., Mangelsdorf D.J. (1999). Structural requirements of ligands for the oxysterol liver X receptors LXRα and LXRβ. Proc Natl Acad Sci U S A *96*, 266-271.

Janowski B.A., Willy P.J., Devi T.R., Falck J.R., Mangelsdorf D.J. (1996). An oxysterol signaling pathway mediated by the nuclear receptor LXRα. Nature *383*, 728-731.

Joseph S.B., Laffitte B.A., Patel P.H., Watson M.A., Matsukuma K.E., Walczak R., Collins J.L., Osborne T.F., Tontonoz P. (2002). Direct and Indirect Mechanisms for Regulation of Fatty Acid Synthase Gene Expression by Liver X Receptors. J Biol Chem *277*, 11019-11025.

Kabashima T., Kawaguchi T., Wadzinski B.E., Uyeda K. (2003). Xylulose 5-phosphate mediates glucose-induced lipogenesis by xylolose 5-phosphate-activated protein phosphatase in rat liver. Proc Natl Acad Sci U S A *100*, 5107-5112.

Kawaguchi T., Osatomi K., Yamashita H., Kabashima T., Uyeda K. (2002). Mechanism for Fatty Acid "Sparing" Effect on Glucose-induced Transcription. J Biol Chem *277*, 3829-3835.

Kawaguchi T., Takenoshita M., Kabashima T., Uyeda K. (2001). Glucose and cAMP regulate the L-type pyruvate kinase gene by phosphorylation/dephosphorylation of the carbohydrate response element binding protein. Proc Natl Sci Acad U S A *98*, 13710-13715.

Lehmann J.M., Kliewer S.A., Moore L.B., Smith-Oliver T.A., Oliver B.B., Su J., Sundseth S.S., Winegar D.A., Blanchard D.E., Spencer T.A., Willson T.M. (1997). Activation of the Nuclear Receptor LXR by Oxysterols Defines a New Hormone Response Pathway. J Biol Chem *272*, 3137-3140.

Li S., Brown M.S., Goldstein J.L. (2010). Bifurcation of insulin signaling pathway in rat liver: mTORC1 required for stimulation of lipogenesis, but not inhibition of gluconeogenesis. Proc Natl Acad Sci U S A *107*, 3441-3446.

Liang G., Yang J., Horton J.D., Hammer R.E., Goldstein J.L., Brown M.S. (2002). Diminished Hepatic Response to Fasting/Refeeding and Liver X Receptor

Agonists in Mice with Selective Deficiency of Sterol Regulatory Element-binding Protein-1c. J Biol Chem *277*, 9520-9528.

Liu Z., Thompson K.S., Towle H.C. (1993). Carbohydrate Regulation of the Rat L-type Pyruvate Kinase Gene Requires Two Nuclear Factors: LF-A1 and a Member of the *c-myc* Family. J Biol Chem *268*, 12787-12795.

Moon Y., Liang G., Xie X., Frank-Kamenetsky M., Fitzgerald K., Koteliansky V., Brown M.S., Goldstein J.L., Horton J.D. (2012). The Scap/SREBP Pathway Is Essential for Developing Diabetic Fatty Liver and Carbohydrate-Induced Hypertriglyeridemia in Animals. Cell Metabolism *15*, 240-246.

Nakagawa T., Ge Q., Pawlosky R., Wynn R.M., Veech R.L., Uyeda K. (2013). Metabolite Regulation of Nucleo-cytosolic Trafficking of Carbohydrate Response Element-binding Protein (ChREBP). J Biol Chem *288*, 28358-28367.

Nohturfft A., DeBose-Boyd R.A., Scheek S., Goldstein J.L., Brown M.S. (1999). Sterols regulate cycling of SREBP cleavage-activating protein (SCAP) between endoplasmic reticulum and Golgi. Proc Natl Acad Sci U S A *96*, 11235-11240.

Ou J., Tu H., Luk A., DeBose-Boyd R.A., Bashmakov Y., Goldstein J.L., Brown M.S. (2001). Unsaturated fatty acids inhibit transcription of the sterol regulatory element-binding protein-1c (SREBP-1c) gene by antagonizing ligand-dependent activation of the LXR. Proc Natl Acad Sci U S A *98*, 6027-6032.

Owen J.L., Zhang Y., Bae S., Farooqi M.S., Liang G., Hammer R.E., Goldstein J.L., Brown M.S. (2012). Insulin stimulation of SREBP-1c processing in transgenic rat hepatocytes requires p70 S6-kinase. Proc Natl Acad Sci U S A *109*, 16184-16189.

Pashkov V., Huang J., Parameswara V.K., Kedzierski W., Kurrasch D.M., Tall G.G., Esser V., Gerard R.D., Uyeda K., Towle H.C., Wilkie T.M. (2011). Regulator of G Protein Signaling (RGS16) Inhibits Hepatic Fatty Acid Oxidation in a Carbohydrate Response Element-binding Protein (ChREBP)-dependent Manner. J Biol Chem *286*, 15116-15125.

Peet D.J., Turley S.D., Ma W., Janowski B.A., Lobaccaro J.A., Hammer R.E., Mangelsdorf D.J. (1998). Cholesterol and Bile Acid Metabolism Are Impaired in Mice Lacking the Nuclear Oxysterol Receptor LXRα. Cell *93*, 693-704.

Poungvarin N, Chang B., Imamura M., Chen J., Moolsuwan K., Sae-Lee C., Li W., Chan L. (2015). Genome-wide Analysis of ChREBP Binding Sites on Male Mouse Liver and White Adipose Chromatin. Endocrinology *156*, 1982-1994.

Radhakrishnan A., Ikeda Y., Kwon H.J., Brown M.S., Goldstein J.L. (2007). Sterol-regulated transport of SREBPs from endoplasmic reticulum to Golgi: Oxysterols block transport by binding to Insig. Proc Natl Acad Sci U S A *104*, 6511-6518.

Repa J.J., Liang G., Ou J., Bashmakov Y., Lobaccaro J.A., Shimomura I., Shan B., Brown M.S., Goldstein J.L., Mangelsdorf D.J. (2000). Regulation of mouse sterol regulatory element-binding protein-1c gene (SREBP-1c) by oxysterol receptors, LXRα and LXRβ. Genes & Development *14*, 2819-2830.

Sakiyama H., Fujiwara N., Noguchi T., Eguchi H., Yoshihara D., Uyeda K., Suzuki K. (2010). The role of *O*-linked GlcNAc modification on the glucose response of ChREBP. Biochem and Biophys Res Comm *402*, 784-789.

Sakiyama H., Wynn R.M., Lee W., Fukasawa M., Mizguchi H., Gardner K.H., Repa J.J., Uyeda K. (2008). Regulation of Nuclear Import/Export of Carbohydrate Response Element-binding Protein (ChREBP). J Biol Chem *283*, 24899-24908.

Seol W., Choi H., Moore D.D. (1995). Isolation of Proteins That Interact Specifically with the Retinoid X .Receptor: Two Novel Orphan Receptors. Molecular Endocrinology *9*, 72-85.

Shimomura I., Shimano H., Horton J.D., Goldstein J.L., Brown M.S. (1997). Differential Expression of Exons 1a and 1c in mRNAs for Sterol Regulatory Element Binding Protein-1 in Human and Mouse Organs and Cultured Cells. J Clin Invest *99*, 838-845.

Song C., Kokontis J.M., Hiipakka R.A., Liao S. (1994). Ubiquitous receptor: A receptor that modulates gene activation by retinoic acid and thyroid hormone receptors. Proc Natl Acad Sci U S A *91*, 10809-10813.

Song C. and Liao S. (2000). Cholestenoic Acid Is a Naturally Occurring Ligand for Liver X Receptor α. Endocrinology *141*, 4180-4184.

Südhof T.C., Russell D.W., Brown M.S., Goldstein J.L. (1987). 42 bp Element from LDL Receptor Gene Confers End-Product Repression by Sterols when Inserted into Viral TK Promoter. Cell *48*, 1061-1069.

Sun L., Seemann J., Goldstein J.L., Brown M.S. (2007). Sterol-regulated transport of SREBPs from endoplasmic reticulum to Golgi: Insig renders sorting signal in Scap inaccessible to COPII proteins. Proc Natl Acad Sci U S A *104*, 6519-6526.

Thompson K.S. and Towle H.C. (1991). Localization of the Carbohydrate Response Element of the Rat L-type Pyruvate Kinase Gene. J Biol Chem *266*, 8679-8682.

Uyeda K. and Repa J.J. (2006). Carbohydrate response element binding protein, ChREBP, a transcription factor coupling hepatic glucose utilization and lipid synthesis. Cell Metabolism *4*, 107-110.

Uyeda K., Yamashita H., Kawaguchi T. (2002) carbohydrate responsive element-binding protein (ChREBP): a key regulator of glucose metabolism and fat storage. Biochem Pharm *63*, 2075-2080.

Wang X., Briggs M.R., Hua X., Yokoyama C., Goldstein J.L., Brown M.S. (1993). Nuclear Protein That Binds Sterol Regulatory Element of Low Density Lipoprotein Receptor Promoter. J Biol Chem *268*, 14497-14504.

Wang X., Sato R., Brown M.S., Hua X., Goldstein J.L. (1994). SREBP-1, a Membrane-Bound Transcription Factor Released by Sterol-Regulated Proteolysis. Cell *77*, 53-62.

Willy P.J., Umesono K., Ong E.S., Evans R.M., Heyman R.A., Mangelsdorf D.J. (1995). LXR, a nuclear receptor that defines a distinct retinoid response pathway. Genes & Development *9*, 1033-1045.

Xu J., Teran-Garcia M., Park J.H.Y., Nakamura M.T., Clarke S.D. (2001). Polyunsaturated Fatty Acids Suppress Hepatic *Sterol Regulatory Element-binding Protein-1* Expression by Accelerating Transcript Decay. J Biol Chem *276*, 9800-9807.

Yamashita H., Takenoshita M., Sakurai M., Bruick R., Henzel W.J., Shillinglaw W., Arnot D., Uyeda K. (2001). A glucose-responsive transcription factor that regulates carbohydrate metabolism in the liver. Proc Natl Acad Sci U S A *98*, 9116-9121.

Ye J., Davé U.P., Grishin N.V., Goldstein J.L., Brown M.S. (2000). Asparagine-proline sequence within membrane-spanning segment of SREBP triggers intramembrane cleavage by Site-2 protease. Proc Natl Acad Sci U S A *97*, 5123-5128.

Yokoyama C., Wang X., Briggs M.R., Admon A., Wu J., Hua X., Goldstein J.L., Brown M.S. (1993). SREBP-1, a Basic-Helix-Loop-Helix-Leucine Zipper Protein That Controls Transcription of the Low Density Lipoprotein Receptor Gene. Cell *75*, 187-197.

Yoshikawa T., Shimano H., Amemiya-Kudo M., Yahagi N., Hasty A.H., Matsuzaka T., Okazaki H., tamura Y., Iizuka Y., Ohashi K., Osuga J., Harada K., Gotoda T., Kimura S., Ishibashi S., Yamada N. (2001). Identification of Liver

X Receptor as an Activator of the Sterol Regulatory Element-Binding Protein 1c Gene Promoter. Mol Cell Bio *21*, 2991-3000.

Zhang Y., Repa J.J., Gauthier K., Mangelsdorf D.J. (2001). Regulation of Lipoprotein Lipase by the Oxysterol Receptors, LXRα and LXRβ. J Biol Chem *276*, 43018-43024.